Permo-Carboniferous extension-related magmatism at the SW margin of the Fennoscandian Shield

K. OBST[1], Z. SOLYOM[2] & L. JOHANSSON[2]

[1]*Institut für Geologische Wissenschaften, Universität Greifswald, F.-L.-Jahn-Strasse 17a, D-17487 Greifswald, Germany (e-mail: obst@uni-greifswald.de)*
[2]*Department of Geology, University of Lund, Sölvegatan 12, S-22362 Lund, Sweden*

Abstract: Permo-Carboniferous rifting in Europe was accompanied by the widespread emplacement of mantle-derived magmas forming regional dyke swarms and sills in northern England, Scotland, Norway and southern Sweden during the late Stephanian and early Autunian. The trends of the dyke swarms intersect at a focal point in the Kattegat south of the Oslo Graben, and are probably all related to a single magmatic centre that could be plume-related. The WNW- to NW-trending dyke swarm at the SW margin of the Fennoscandian Shield in southern Sweden is composed mainly of tholeiitic dolerites, with lesser amounts of alkaline mafic rocks (camptonites, alkali basalts and spessartites) and trachytes. The alkaline mafic rocks are enriched in Ba, Sr, Nb, P and CO_2, implying a metasomatic enrichment of their upper-mantle source prior to melting. After generation of alkaline melts by relatively small degrees of partial melting, increased extension was accompanied by the formation of subalkaline tholeiitic magmas. Whole-rock compositions (Mg-numbers between 55 and 30) and mineral chemistry (olivine Fo_{60}–Fo_{40}; clinopyroxene approximately $Wo_{30}En_{45}Fs_{15}$; plagioclase An_{70}–An_{50}) indicate relatively evolved melts that have undergone crystal fractionation of olivine and clinopyroxene. Two groups of dolerites can be distinguished on the basis of bivariate element plots, e.g. Zr–TiO_2 and La–Sm. Although both groups show enrichment in the whole range of incompatible trace elements, slight differences in mantle-normalized trace-element patterns and different Nb/La ratios suggest that they were generated from two different sources. Group I dolerites were formed from a (re-)enriched, but isotopically mildly depleted, sublithospheric garnet-bearing mantle source (Nb/La mostly > 0.9, $\varepsilon Nd_i = +4$ to $+3$, where εNd_i is the initial Nd isotope ratio), whereas group II dolerites seem to indicate mixing of the asthenospheric-derived magmas with lithospheric mantle melts (Nb/La mostly < 0.9, $\varepsilon Nd_i = 0$ to -1). Increasing Th/Ta ratios together with decreasing U/Nb ratios from group I towards group II dolerites further reflect progressive crustal contamination.

Regionally extensive dyke swarms represent paths of magma transport from the upper mantle to high levels in the Earth's crust, and provide evidence for regional extension. Such dyke swarms often have consistent orientations over long distances, indicative of the orientation of the regional stress field during intrusion. They are genetically related to extensional tectonics coupled with asthenospheric upwelling or rising mantle plumes, which may lead to the formation of large igneous provinces (LIPs) and the break-up of continental lithosphere (Ernst & Buchan 1997).

Late Carboniferous and Permian times were characterized by block faulting and basin formation in central and western Europe (e.g. Ziegler 1990). Sedimentation was often combined with igneous activity, especially in Scotland (Francis 1991), the Oslo Graben, Norway (Neumann 1994; Sundvoll & Larsen 1995) and the NE German Basin (Benek *et al.* 1996). Continental rifting was accompanied by the intrusion of sill complexes and regional dyke swarms (Fig. 1) which trend approximately E–W in the Midland Valley of Scotland (Francis 1978), WNW–ESE to NW–SE in southern Sweden (Bergström 1985), and mainly N–S to NNW–SSE in the Oslo region (Ramberg & Larsen 1978).

Field observation and aeromagnetic data of the Swedish Geological Survey (SGU) demonstrate the existence of thousands of WNW- to NW-trending dykes, with various thicknesses and lengths, in the southernmost Swedish province of Scania. They intrude granites and gneisses of the Precambrian basement and the overlying Lower Palaeozoic sediments. Palaeomagnetic and radiometric age determinations

From: WILSON, M., NEUMANN, E.-R., DAVIES, G.R., TIMMERMAN, M.J., HEEREMANS, M. & LARSEN, B.T. (eds) *Permo-Carboniferous Magmatism and Rifting in Europe*. Geological Society, London, Special Publications, **223**, 259–288. 0305-8719/04/$15

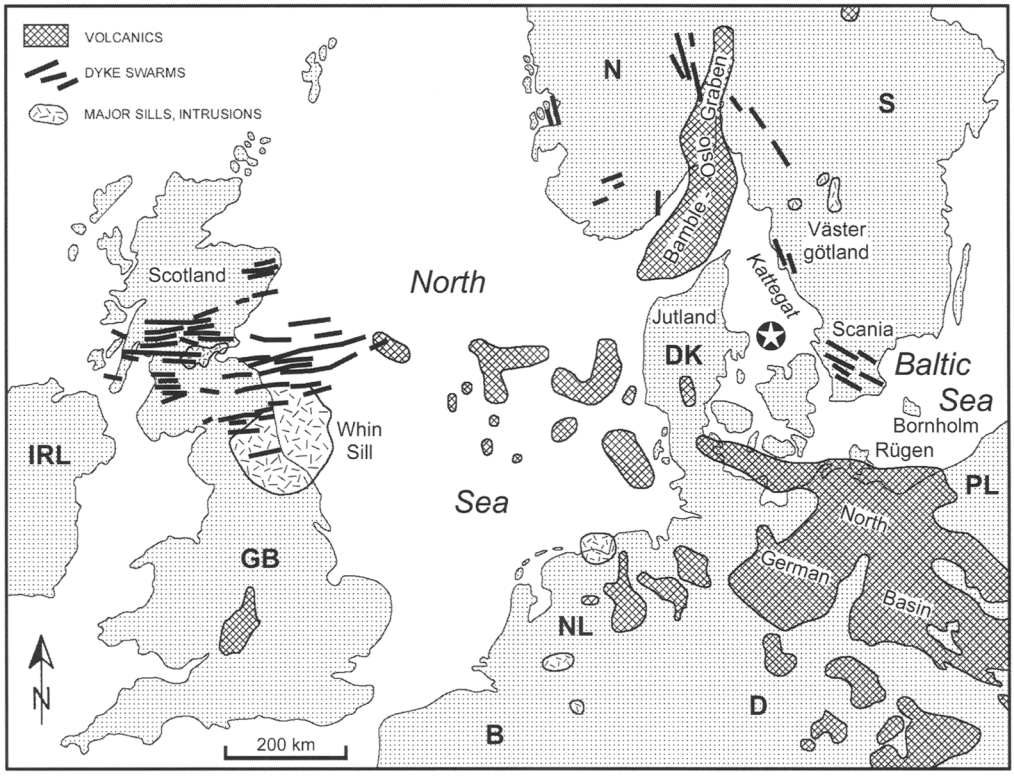

Fig. 1. Distribution of Permo-Carboniferous igneous rocks in central and western Europe (based on Ziegler 1990). A possible location for a magmatic centre (plume head?) that could have fed the regional dyke swarms of Scotland, the Oslo region and Scania is marked by the star in the Kattegat near the Silkeborg Gravity High (cf. Thybo *et al.* 1990). B, Belgium; D, Germany; DK, Denmark; GB, Great Britain; IRL, Ireland; N, Norway; NL, the Netherlands; PL, Poland; S, Sweden.

(Bylund 1974; Klingspor 1976) indicate that most of the intrusions are contemporaneous with the widespread magmatic activity that occurred in central Europe between 300 and 290 Ma. The overwhelming majority of the dykes are tholeiitic dolerites (>90–95%), but there are also alkaline mafic and trachytic dykes (Obst 1999). The Scania dyke swarm extends to the SE on the Danish island of Bornholm (Fig. 1), as indicated by a few WNW- and NW-striking dykes with similar geochemical characteristics (Obst 2000).

This study focuses on the geochemistry, petrogenesis and the geotectonic setting of the mafic rocks of the Scania dyke swarm and their correlatives in northern Germany. Their geochemical characteristics are compared with mafic rocks of similar age from northern England and the Midland Valley of Scotland, and Västergötland in central Sweden. The formation of the associated trachytic rocks is considered briefly.

Geological setting of the dyke swarm

The SW margin of the Fennoscandian Shield

Pre-existing zones of weakness, such as large detachments, thrust zones or terrane boundaries separating lithospheric domains of different thickness and structure, often determine the location of dyke swarms. Geophysical data show a change in thickness of the present-day crust, as well as of the whole lithosphere, between southern Sweden and northern Germany (Blundell 1992). The crustal thickness decreases gradually from 45 km below the Fennoscandian Shield to 30 km below Denmark and the North German Basin (Fig. 2b). Similar differences in the structure of the lithosphere are likely to have existed since Late Carboniferous and Permian times (see Pascal *et al.* 2004).

The SW margin of the Fennoscandian Shield is marked by a number of distinct tectonic structures, which are part of a fault zone extending from the North Sea to the Black

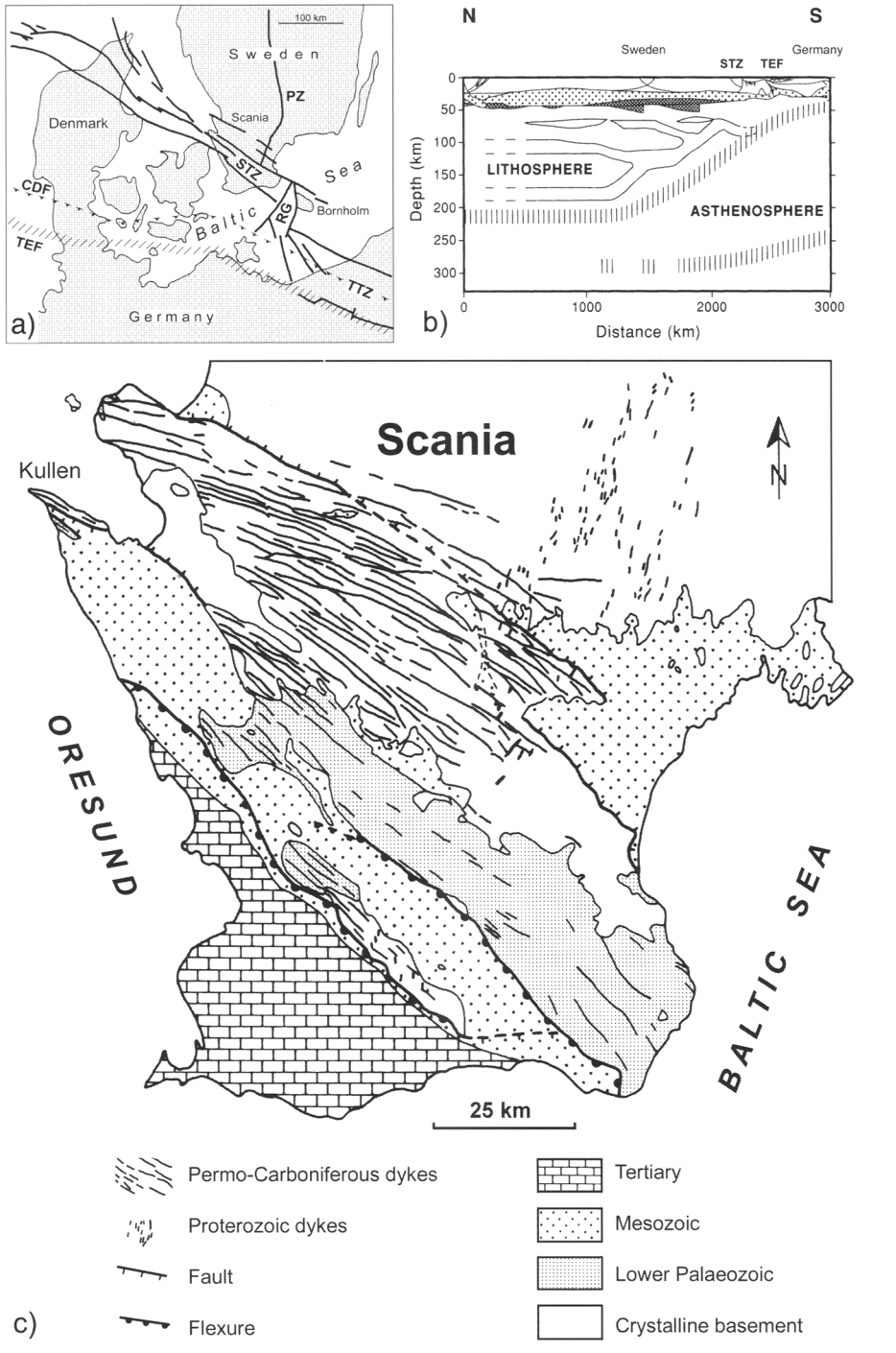

Fig. 2. (**a**) Fault pattern along the SW margin of the Fennoscandian Shield (Berthelsen 1992, modified), (**b**) profile through the lithosphere between Sweden and Germany based on seismic investigations (Blundell 1992; sedimentary bedrock and granitic upper crust, white; granulitic lower crust, stipple; underplated mafic rocks, dark grey; base of the lithosphere and asthenosphere, hatched line) and (**c**) geological map of Scania (SGU 1988, simplified).

Sea. A NW branch, the Sorgenfrei–Tornquist Zone (STZ), is separated from the SE Tornquist–Teisseyre Zone (TTZ) by an off-set at the Rønne Graben (RG) west of Bornholm (Fig. 2a). The TTZ is considered to mark the SW border of the East European Craton, while the STZ separates the Fennoscandian Shield in the NE from the 'Danish Massif' in the SW, which belongs to the ancient crust of eastern Europe as documented in drill cores. In the west the border with the accreted younger terranes of central Europe is situated further south, defined by the nearly E–W-trending Trans-European Fault (TEF) or Trans-European Suture Zone (TESZ). The exact position of this suture is open to discussion, dependent on the geophysical measurements used for its determination (Dadlez 1997; Hoffmann *et al.* 1998; Gossler *et al.* 1999). Drill cores only document the extension of the Caledonian Deformation Front (CDF), which itself marks the northern extension of an accretionary wedge between the palaeocontinent of Baltica and the terrane Avalonia formed during the Caledonian orogeny and thrust onto the Fennoscandian Shield (cf. Katzung 2001).

Orientation, geometry of the Scania dykes and amount of crustal dilation

In southern Sweden a large WNW- to NW-striking regional dyke swarm, predominantly situated within the STZ at the SW margin of the Fennoscandian Shield, has been linked to lithospheric extension during the Late Palaeozoic (Gorbatschev *et al.* 1987). Numerous dykes form this swarm within a *c.* 70 km-wide zone, which is also marked by intense Mesozoic block faulting resulting in NW–SE-oriented horst and graben structures (Fig. 2). The dykes are mostly vertical and cut both crystalline basement and overlying Cambro-Silurian sediments. They generally strike WNW–ESE to NW–SE, although some dykes follow E–W-oriented directions in the basement (Bergström 1985). Their thickness ranges from a few metres to more than 50 m, with a few intrusions reaching 100 m. Based on aeromagnetic studies, the dykes probably represent the intrusion of a magma volume of at least 4000 km^3. This estimate was made by Henkel & Sundin (1979), assuming about 6% total extension. They also postulated that the E–W-trending dykes are older than those oriented NW–SE, but this has not been confirmed on basis of detailed field studies (Obst 1999).

Structural investigations (Obst & Katzung 2004) indicate that dyke formation in Scania is related to extension processes without large-scale horizontal or vertical movements; only slight rotations of small basement blocks can be demonstrated. The dykes generally form a braided but slightly curved pattern converging towards the NW (Fig. 2). Distribution analyses suggest that the mean orientation of the dykes changes from WNW–ESE in the NW part of the dyke swarm to NW–SE in the SE part. The direction of the least compressive stress ($\sigma 3$) varies between NNE–SSW and NE–SW. Furthermore, field studies indicate that the amount of extension increases from the SE (0.6%) to the NW (2.5%) parts of the dyke swarm. This corresponds to an increasing number of dykes and the occurrence of a more variable dyke geometry in the part proximal to a possible magmatic centre beneath the Kattegat. Remnants of such a centre could be indicated by the presence of a large mafic body in the lower crust near Silkeborg on the Danish peninsula Jutland (Thybo *et al.* 1990). The Silkeborg Gravity High is a pronounced anomaly that extends over a 50 km distance, probably caused by a batholith in the crystalline basement. This magmatic centre could have fed the time-equivalent dyke swarms and sill complexes of Scania, northern England, Scotland and the Oslo Rift.

Petrography of the dykes in the Sorgenfrei–Tornquist Zone

Three different types of dykes can be distinguished within the Scania dyke swarm. The majority consist of dolerites, mostly quartz-bearing. Subordinate alkaline mafic rocks and reddish-coloured intrusions with trachytic texture and composition also occur. Detailed petrographic descriptions of the dykes are given by Obst (1999).

The *dolerite* dykes typically have chilled margins, and are fine–medium-grained; the central part of the thicker dykes are coarse-grained. They show either an ophitic–subophitic or intergranular texture; a few are plagioclase-phyric. The major minerals are lath-shaped plagioclase, which occurs in two, sometimes three, generations, and augite. Opaques (titanomagnetite and ilmenite), hornblende and biotite also occur, and apatite is an important accessory mineral. Quartz occurs commonly as intergrowths with alkali feldspar, sometimes filling the interstices between the major minerals. These quartz-bearing dykes were originally called the Konga diabases (Törneboom 1877). The plagioclase is often sericitized and the pyroxene partially chloritized. Pseudomorphs after olivine can be identified in only a few dykes. The olivine

is commonly replaced by serpentine and calcite; fresh cores are rarely preserved. Calcite and chlorite are common fillings of amygdales. Thin intrusions, which commonly strike obliquely to the 'normal-type' dolerite dykes, show a greater abundance of amygdales. Another unusual dolerite type is exposed east of Öved in central Scania, which probably forms an intrusive body (sill?) elongated NW–SE. This reddish-brown rock is also mainly composed of plagioclase, pyroxene and opaques, but contains a higher amount of olivine, which is completely altered, mostly into an iron-bearing phase. The opaque pseudomorphs after olivine, as well as the remarkable colour, suggest extensive hydrothermal alteration. Amygdales, filled with calcite, chlorite and chalcedony, seem to be concentrated in the upper part of the outcrop.

The *alkaline mafic rocks* have a very different mineralogy from the dolerites. Mafic dykes with olivine and Ti-rich pyroxene phenocrysts, set in a fine-grained groundmass, were reported from an area near Tolånga in central Scania and described as porphyritic melaphyres (Hadding 1916). They intrude Early Palaeozoic sediments. Similar rocks were found nearby in a quarry at the small basement horst named Torpa Klint, where they form a set of narrow dykes (Hjelmqvist 1939). They all are characterized by variable amount of hydrous minerals, and their petrographic characteristics allow a subdivision into camptonites, basaltic camptonites and alkali basalts according to the classification of Rock (1991). The phenocrysts are commonly altered, especially the olivine, which is strongly serpentinized or replaced by calcite and chlorite. Rarely, tiny crystals of chrome spinel are observed, mostly occurring as idiomorphic inclusions in olivine. Brownish hornblende frequently forms microphenocrysts. A second generation of chloritized clinopyroxene, plagioclase and opaques occurs within the brownish devitrified groundmass. Biotite is rare, apatite is a common accessory, subordinate nepheline fills the intersticies. Most of the dykes have conspicuous amygdales filled with calcite, chlorite, quartz and zeolites (analcime), commonly forming amygdale-rich bands. Also typical are felsic ocelli, mainly consisting of feldspar, amphibole and biotite. A dyke of alkali basaltic composition was also found at the western coast of Scania, near Nyhamnsläge south of the Kullen horst (Obst 1999). Furthermore, inclined or sheet-like dykes that contain small hornblende phenocrysts in a matrix of alkali feldspar, chlorite and carbonate are known from the NW edge of the Kullen horst. They are classified as spessartites (Obst 1999), and considered to belong to the group of alkaline mafic intrusions.

The third type of dykes are *trachytic* and are named 'kullaites' after their type locality, the Kullen horst (Hennig 1899; Hjelmqvist 1930). These reddish-grey or -brown, partly bright red, rocks have a distinctive trachytic texture. Feldspar phenocrysts, mostly plagioclase, occur in a crystalline matrix of plagioclase–alkali feldspar laths. The interstices are commonly filled with secondary chlorite and calcite, but opaques and quartz also occur. In some rocks biotite and altered pyroxene microphenocrysts form minor constituents. One dyke of similar composition, exposed in the quarry of Torpa Klint (central Scania), has been described as porphyritic syenite (Hjelmqvist 1939). The rock contains large phenocrysts of alkali feldspar and biotite, but due to overall petrographic and geochemical similarities it can be regarded as belonging to the trachytic group (Obst 1999). Trachytic schlieren of similar composition also occur in some of the alkaline mafic dykes.

Mineral chemistry of the mafic dykes

Electron microprobe analyses

Several hundred microprobe analyses on eight dolerites and four alkaline mafic rock samples were performed at the Geochemical Laboratory of the University of Göttingen, using a JEOL XA 8900 RL equipped with five wavelength dispersive spectrometers. Operating conditions for routine mineral analysis were 15 kV, 12–15 nA beam current, with 15–30 s counting time on the peak of all measured elements. On average, 10–25 analyses were performed on each mineral in all samples. For the purpose of determining the extent of zonation, traverses were made across individual mineral grains. Raw data were corrected using the CITZAF procedure of Armstrong (1995). Representative mineral analyses are given in Table 1.

Dolerites

Three samples were chosen from dolerites with olivine pseudomorphs (Sk 26, Sk 27 and Sk 70). One sample was taken from a plagioclase-phyric dolerite (Sk 94). The other four samples represent common quartz-bearing dolerites with intergranular texture (Sk 98, Sk 108, Sk 130 and Sk 132).

Most of the dolerites lack *olivine* and, if crystals occur, they are completely altered. Only the dolerite dyke of Örnahusen (Sk 70) exposed on the SE coast of Scania contains relatively fresh remnants of olivine. Measurements across

Table 1. *Representative analyses of major and minor minerals in the Scania dolerites (D), camptonites (C) and spessartites (S).* **Core and* †*rim analyses for a single crystal:* **(a)** *spinel (sp), olivine (ol), pigeonite (pig);* **(b)** *clinopyroxene (cpx);* **(c)** *(ilmenite) il titanomagnetite (tm);* **(d)** *plagioclase (pl) and feldspar (fsp); and* **(e)** *amphibole (am) and biotite (bt).*

(a)	sp	sp	ol	ol	ol*	ol†	ol	ol	ol*	ol†	pig
Rock type	C	C	C	C	D	D	D	D	D	D	D
Sample	Sk 121	Sk 121	Sk 121	Sk 121	Sk 70	Sk 70	Sk 70	Sk 70	Sk 70	Sk 70	Sk 70
SiO_2	0.12	0.13	39.55	39.03	36.11	33.41	35.13	34.74	34.47	32.39	52.05
TiO_2	0.43	0.39									0.38
$Al2O_3$	17.44	26.28	0.03	0.06	0.02	0.02	0.02	0.00	0.00	0.01	0.70
$Cr2O_3$	50.31	39.66									0.02
FeO	15.22	16.08	17.95	19.34	35.63	48.99	40.60	41.99	46.21	54.72	21.36
MnO	0.18	0.17	0.35	0.40	0.48	0.75	0.54	0.62	0.65	0.80	0.48
NiO	0.16	0.21	0.13	0.10	0.07	0.04	0.07	0.08	0.05	0.02	0.00
MgO	15.25	16.27	42.12	40.43	27.92	16.66	23.50	22.51	19.27	11.79	20.43
CaO			0.24	0.23	0.25	0.33	0.25	0.24	0.27	0.29	4.13
Na_2O											0.09
Total	99.11	99.18	100.37	99.60	100.49	100.19	100.11	100.17	100.92	100.01	99.63
Mg#			80.70	78.84	58.28	37.74	50.78	48.86	42.64	27.75	63.03

(b)	cpx	cpx	cpx	cpx	cpx	cpx	cpx	cpx	cpx	cpx	cpx	cpx
Rock type	D	D	D	D	D	D	D	D	D	D	D	D
Sample	Sk 26	Sk 26	Sk 27	Sk 27	Sk 70	Sk 70	Sk 94	Sk 94	Sk 98	Sk 98	Sk 108	Sk 108
SiO_2	52.37	51.70	52.51	51.01	51.53	50.82	48.64	50.39	51.02	51.16	50.93	51.01
TiO_2	0.66	0.71	0.56	1.01	0.93	0.97	1.58	1.40	0.79	0.85	0.84	0.70
Al_2O_3	2.04	2.31	1.56	2.22	1.69	1.72	4.77	2.95	1.43	1.55	1.81	1.42
Cr_2O_3	0.22	0.09	0.25	0.05	0.15	0.00	0.43	0.03	0.01	0.02	0.00	0.03
FeO	7.64	8.75	8.83	11.41	10.70	15.60	10.77	11.31	15.96	14.30	11.86	14.12
MnO	0.14	0.24	0.30	0.29	0.24	0.39	0.19	0.26	0.38	0.36	0.33	0.54
MgO	17.16	16.63	18.11	15.73	16.60	14.99	14.81	14.75	13.97	14.65	15.33	13.57
CaO	19.26	18.69	17.37	17.54	17.63	15.10	17.99	18.31	16.15	16.61	17.91	18.04
Na_2O	0.24	0.19	0.23	0.25	0.21	0.15	0.34	0.39	0.27	0.30	0.24	0.27
K_2O	0.02	0.00	0.00	0.01	0.00	0.00	0.00	0.00	0.00	0.00	0.00	0.00
Total	99.75	99.30	99.72	99.52	99.68	99.74	99.52	99.78	99.97	99.79	99.25	99.70
Mg#	80.01	77.21	78.52	71.08	73.44	63.14	71.02	69.92	60.94	64.62	69.73	63.14
en	0.47	0.46	0.50	0.44	0.46	0.42	0.41	0.41	0.41	0.39	0.43	0.38
fs	0.10	0.12	0.11	0.15	0.14	0.23	0.13	0.15	0.20	0.23	0.16	0.20
wo	0.35	0.34	0.32	0.32	0.32	0.28	0.29	0.33	0.31	0.30	0.33	0.34

	cpx	cpx	cpx	cpx	cpx*	cpx†	cpx*	cpx†	cpx	cpx	cpx	cpx
Rock type	D	D	D	D	C	C	C	C	C	C	C	C
Sample	Sk 130	Sk 130	Sk 132	Sk 132	Sk 116	Sk 116	Sk 116	Sk 116	Sk 121	Sk 121	Sk 122	Sk 122
SiO_2	50.91	50.78	51.13	51.06	50.06	46.95	48.03	41.72	50.45	47.44	48.83	47.51
TiO_2	1.04	1.04	0.78	0.96	0.67	1.14	1.15	2.77	0.96	1.54	1.23	1.27
Al_2O_3	2.48	2.26	2.14	2.25	5.04	8.40	7.46	11.80	4.45	7.62	6.06	8.70
Cr_2O_3	0.11	0.02	0.03	0.02	0.40	0.20	0.09	0.02	0.40	0.86	0.04	0.06
FeO	9.89	11.93	11.48	11.92	4.75	5.62	5.49	8.25	4.87	5.49	6.11	6.22
MnO	0.22	0.31	0.33	0.35	0.11	0.08	0.12	0.14	0.12	0.09	0.10	0.15
MgO	16.15	15.29	16.05	15.70	15.38	13.13	13.76	10.41	15.54	13.57	14.17	13.16
CaO	18.65	17.67	17.54	16.88	22.78	23.10	23.19	23.19	22.89	22.92	22.84	22.26
Na_2O	0.24	0.30	0.26	0.30	0.40	0.39	0.38	0.37	0.28	0.39	0.29	0.58
K_2O	0.01	0.00	0.01	0.00	0.02	0.01	0.00	0.01	0.00	0.01	0.01	0.00
Total	99.70	99.61	99.74	99.43	99.61	99.02	99.67	98.67	99.96	99.92	99.68	99.91
Mg#	74.43	69.55	71.36	70.13	85.23	80.64	81.71	69.22	85.05	81.50	80.52	79.04
en	0.45	0.43	0.45	0.44	0.42	0.36	0.38	0.29	0.42	0.37	0.39	0.36
fs	0.12	0.16	0.14	0.17	0.03	0.03	0.04	0.04	0.04	0.04	0.05	0.05
wo	0.33	0.32	0.31	0.31	0.38	0.35	0.36	0.30	0.39	0.35	0.37	0.33

Table 1. *Continued.*

(c)	il	il	il	il	il	il	il	il
Rock type	D	D	D	D	D	D	D	D
Sample	Sk 26	Sk 27	Sk 70	Sk 94	Sk 98	Sk 108	Sk 130	Sk 132
SiO_2	0.00	0.00	0.00	0.00	0.01	0.00	0.00	0.00
TiO_2	49.42	49.67	50.11	48.78	49.34	48.03	47.91	49.62
Al_2O_3	0.08	0.04	0.05	0.04	0.03	0.04	0.02	0.05
Cr_2O_3	0.05	0.02	0.03	0.05	0.02	0.03	0.04	0.03
FeO	48.21	47.52	46.46	48.41	47.75	48.57	49.09	46.20
MnO	0.56	0.45	0.51	1.41	1.41	0.65	0.86	2.46
MgO	0.46	0.70	1.57	0.00	0.00	0.59	0.27	0.01
CaO	0.02	0.00	0.01	0.06	0.13	0.02	0.07	0.32
Na_2O	0.00	0.00	0.00	0.00	0.02	0.01	0.05	0.00
K_2O	0.00	0.01	0.00	0.00	0.00	0.00	0.00	0.00
Total	98.80	98.42	98.74	98.75	98.71	97.94	98.30	98.69
Fe^{2+}	0.88	0.78	0.79	1.03	0.86	1.23	1.30	0.76
Fe^{3+}	7.31	7.31	7.03	7.22	7.28	7.07	7.07	7.11

	tm	tm	tm	tm	tm	tm	tm	tm
Rock type	D	D	D	D	D	D	D	S
Sample	Sk 26	Sk 27	Sk 70	Sk 94	Sk 98	Sk 130	Sk 132	Sk 142
SiO_2	0.08	0.08	0.04	0.03	0.10	0.09	0.02	0.03
TiO_2	26.72	20.98	21.77	12.77	17.35	9.51	14.02	17.14
Al_2O_3	1.48	2.46	2.11	1.36	1.14	0.76	1.05	2.92
Cr_2O_3	0.11	0.10	0.04	0.12	0.07	0.23	0.06	0.02
FeO	65.41	68.84	71.09	78.95	74.89	82.27	77.35	71.05
MnO	1.06	1.87	0.58	0.51	0.71	0.41	0.86	0.59
MgO	0.00	0.00	0.42	0.02	0.00	0.04	0.05	0.00
CaO	0.04	0.02	0.00	0.07	0.10	0.07	0.10	0.13
Na_2O	0.00	0.06	0.00	0.04	0.04	0.00	0.00	0.03
K_2O	0.01	0.00	0.02	0.00	0.00	0.00	0.00	0.03
Total	94.90	94.41	96.05	93.87	94.39	93.37	93.50	91.94
Fe^{2+}	2.97	5.38	5.34	9.57	7.49	11.19	9.05	6.84
Fe^{3+}	13.94	12.31	12.61	10.76	11.79	10.09	10.99	11.79

(d)	pl	pl*	pl†	pl*	pl†	pl*	pl†
Rock type	D	D	D	D	D	D	D
Sample	Sk 27	Sk 26	Sk 26	Sk 70	Sk 70	Sk 94	Sk 94
SiO_2	50.81	52.65	57.19	52.19	56.42	50.03	53.34
TiO_2	0.09	0.03	0.13	0.15	0.02	0.06	0.11
Al_2O_3	29.73	28.50	25.71	29.04	26.35	30.41	28.52
Cr_2O_3	0.00	0.00	0.00	0.00	0.00	0.01	0.01
FeO	0.73	0.84	0.79	0.75	0.86	0.62	0.73
MnO	0.03	0.01	0.00	0.03	0.01	0.01	0.00
MgO	0.17	0.14	0.04	0.13	0.05	0.13	0.13
CaO	13.64	12.09	8.36	12.80	9.12	13.93	12.11
Na_2O	3.65	4.35	6.49	4.10	6.06	3.40	4.66
K_2O	0.11	0.16	0.32	0.23	0.42	0.20	0.28
Total	98.95	98.77	99.03	99.42	99.32	98.80	99.90
an	66.93	60.00	40.81	62.46	44.30	68.56	58.00
ab	32.41	39.07	57.32	36.21	53.26	30.28	40.39
or	0.65	0.93	1.87	1.33	2.44	1.16	1.61

Table 1. *Continued.*

	pl	pl*	pl†	pl*	pl†	pl*	pl†
Rock type	D	D	D	D	D	D	D
Sample	Sk 98	Sk 108	Sk 108	Sk 130	Sk 130	Sk 132	Sk 132
SiO_2	53.73	54.20	55.34	52.36	57.11	52.06	57.57
TiO_2	0.10	0.08	0.06	0.08	0.06	0.07	0.05
Al_2O_3	27.65	27.50	26.59	29.01	26.07	28.80	25.82
Cr_2O_3	0.00	0.00	0.02	0.03	0.02	0.03	0.03
FeO	0.81	0.67	0.50	0.76	0.38	0.71	0.51
MnO	0.00	0.00	0.00	0.00	0.00	0.03	0.06
MgO	0.11	0.11	0.05	0.13	0.02	0.15	0.04
CaO	11.13	10.64	9.45	12.40	8.43	12.48	8.14
Na_2O	5.24	5.20	5.80	4.32	6.50	4.20	6.64
K_2O	0.30	0.30	0.34	0.16	0.34	0.24	0.52
Total	99.06	98.70	98.15	99.25	98.93	98.77	99.38
an	53.09	52.15	46.43	60.76	40.93	61.28	39.18
ab	45.23	46.12	51.56	38.30	57.10	37.32	57.84
or	1.68	1.74	2.01	0.94	1.97	1.40	2.98

	fsp	fsp	fsp	fsp	fsp	fsp	fsp
Rock type	C	C	C	C	C	S	S
Sample	Sk 116	Sk 121	Sk 121	Sk 122	Sk 122	Sk 142	Sk 142
SiO2	67.13	50.90	51.13	55.72	61.41	61.77	64.61
TiO2	0.02	0.11	0.08	0.06	0.06	0.09	0.06
Al2O3	19.75	29.93	29.12	27.06	23.00	19.62	18.62
Cr2O3	0.01	0.00	0.00	0.02	0.00	0.00	0.02
FeO	0.21	0.88	1.50	0.31	0.21	1.03	0.40
MnO	0.01	0.00	0.01	0.00	0.02	0.04	0.02
MgO	0.02	0.14	0.66	0.04	0.01	0.44	0.04
CaO	0.47	12.73	9.84	9.12	4.47	2.26	0.13
Na2O	11.29	3.91	3.31	5.80	8.25	7.64	4.10
K2O	0.16	0.38	2.20	0.41	1.08	3.80	10.51
Total	99.08	98.97	97.85	98.53	98.51	96.68	98.51
an	2.24	62.85	53.33	45.37	21.61	10.97	0.63
ab	96.86	34.93	32.47	52.22	72.18	67.08	36.98
or	0.90	2.22	14.20	2.41	6.20	21.96	62.39

(e)	am	am	am	am	am	am	bt
Rock type	D	D	S	S	C	C	D
Sample	Sk 27	Sk 98	Sk 142	Sk 142	Sk 116	Sk 116	Sk 130
SiO_2	50.09	44.09	38.29	37.54	37.39	38.43	37.44
TiO_2	0.75	1.26	6.55	6.40	2.54	1.92	3.65
Al_2O_3	4.20	5.85	12.95	13.70	15.63	14.86	11.58
Cr_2O_3	0.00	0.02	0.03	0.03	0.00	0.05	0.043
FeO	24.38	25.77	9.71	11.23	14.10	14.88	23.4
MnO	0.16	0.34	0.12	0.16	0.33	0.40	0.125
MgO	7.21	7.39	13.00	12.11	10.54	10.21	10.78
CaO	10.12	9.38	11.67	11.81	11.37	11.66	0.017
Na_2O	0.93	1.97	2.55	2.45	2.43	2.52	0.301
K_2O	0.50	0.78	1.16	1.21	1.12	1.13	8.62
Total	98.34	96.84	96.04	96.64	95.45	96.06	95.956
Mg#	34.52	33.83	70.47	65.78	57.13	55.02	

Normative minerals: ab, albite; *an*, anorthite; *en*, enstatite; *fs*, ferrosillite; *or*, orthoclase; *wo*, wollastonite.
Mg#, Mg number (see text for details).

several olivine crystal yielded values approximately between Fo_{60} and Fo_{40}; there is some zoning to Fe-rich rims ($\leq Fo_{40}$). The relatively low Mg numbers (where Mg number = mole% Mg/(Mg + Fe)) indicate that olivine crystallized from a relatively evolved melt.

Clinopyroxene in the dolerites is mostly augite (mean approximately $Wo_{30}En_{45}Fs_{15}$), and line scans show only minor scattering variations in major oxide distribution (patchy zoning). The data are plotted in Figure 3. Interestingly, three analyses from the Örnahusen dyke (Sk 70) are pigeonite.

Larger and nearly idiomorphic *plagioclase* crystals in the dolerites with olivine pseudomorphs (Sk 26, Sk 27 and Sk 70) and the phenocrysts of the plagioclase-phyric dyke from Arild at the northern coast of the Kullen horst (Sk 94) show a range in composition from An_{70} to An_{55}. Line scans indicate slight compositional fluctuations, which correspond with zonations visible under the microscope or in back-scattered images. Only the outermost rims of these plagioclase laths sometimes show a different composition, $\leq An_{50}$, equal to the plagioclase composition of the second generation. The plagioclase crystals in the quartz-bearing dolerites (Sk 98, Sk 108, Sk 130 and Sk 132) have mostly a composition between An_{65} and An_{50}, and have albite-rich rims.

Fe–Ti oxide analyses show a range in ulvöspinel content of magnetite and a more limited range in composition of coexisting ilmenite. This is probably due to variable degrees of re-equilibration of the oxides and, in addition, the reaction between oxides and adjacent silicates during cooling of the magmas. The MgO content of magnetite is always below 0.5%. This is interpreted to show that magnetite did not crystallize in equilibrium with olivine or other Mg-silicates. The low levels of haematite in the ilmenite analyses are probably close to the primary composition, which for most tholeiites is less than 10–15 mol% (Frost & Lindsley 1991). The geikeilite component is often very low, indicative of late-stage or secondary alteration processes.

Tiny crystals of *amphibole* occur in the groundmass of nearly all dolerites. They are typically ferropargasite (Leake *et al.* 1997). Occurrences of *biotite* in the dolerites are rare, but they mostly have approximately equal contents of phlogopite and annite components.

Alkaline mafic rocks

Three samples from camptonites in central Scania (Sk 116, Sk 121 and Sk 122) and one from a spessartite in NW Scania (Sk 142) were selected for mineral chemistry investigations.

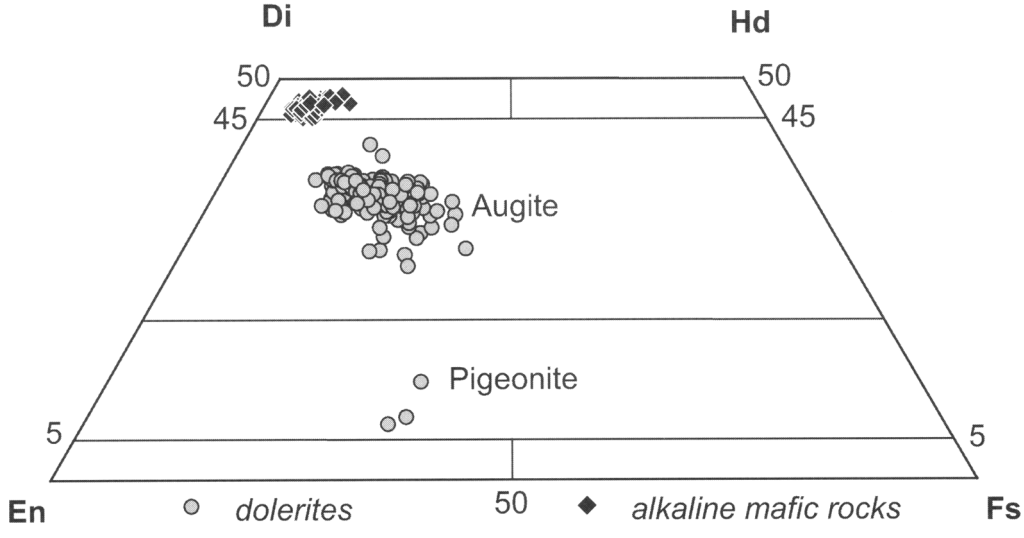

Fig. 3. Microprobe analyses of pyroxenes plotted in the pyroxene quadilateral to show compositional differences between the Scania tholeiitic dolerites and the alkaline mafic rocks (camptonites). Di, diopside; Eu, eustatite; Fs, ferrosillite; Hd, hedenbergite.

The alkaline mafic rocks generally show differences in mineral composition compared to the tholeiites, but also internally.

Fresh *olivine* remants in partly altered grains, only found in a narrow camptonite dyke from the Torpa Klint quarry in central Scania (Sk 121), have Mg numbers of about Fo_{80} indicating that these melts are much closer to primary compositions. Tiny *spinel* inclusions are Mg–Al chromites.

Clinopyroxene phenocrysts in several camptonite dykes are diopsidic (Fig. 3). Zonation is indicated by a decreasing Mg number from core to rim, while the tschermak component increases. Ti-rich rims are also typical (up to 3% TiO_2).

The rare *magnetite* has low–medium contents of ulvöspinel, but contain relatively high amounts of the haematite component, especially in the camptonites.

Amphibole phenocrysts in the spessartite are kaersutite with relatively high amounts of TiO_2 (more than 6%). Amphibole microphenocrysts in the camptonites have a different composition (e.g. lower content of TiO_2; less than 3%), and are pargasite.

Analyses of small *feldspar* crystals in the spessartite indicate a variable mixture, mostly of albite and orthoclase, while the feldspar crystals in the groundmass of the camptonites are either plagioclase or alkali feldspar with a varying amount of the orthoclase component between 2 and 15%.

Bulk rock chemistry

Sampling and analytical procedures

Samples of dykes from all parts of the swarm exposed in quarries, road-cuts and coastal areas were collected. Apart from the chilled margins, the dolerite dykes commonly appear homogeneous and show no zoning or other macroscopic features of internal differentiation. 2 to 5 kg samples were taken as pieces or blocks distributed over the exposures. Only in a few cases of very wide dykes were samples of the marginal zone also taken. 86 dolerite samples and 30 samples from alkaline dykes were analysed partly in Lund and partly in Hannover. A detailed description of the analysis procedures are given in Obst (1999). To improve the database, especially for trace-element concentrations, samples of 35 dolerite dykes from Scania and, in addition, six samples from two dolerite sills in Västergötland were reanalysed at the Bundesanstalt für Geowissenschaften und Rohstoffe Hannover using a wavelength dispersive X-ray fluorescence (XRF) machine (Philips) and an inductively coupled plasma-mass spectrometer (ICP-MS) ELAN 5000A (Perkin Elmer). These new data are reported in Table 2; the sample locations are given in Table 3.

For the *XRF analyses* 1 g of homogenized powder was heated to 1030 °C to calculate the loss on ignition (LOI). Then, the material was mixed with $LiBO_2$ in the proportion 1:5 before producing glass beads by melting this mixture. Ten major elements (SiO_2, TiO_2, Al_2O_3, $Fe_2O_3^*$ (as total iron), MnO, MgO, CaO, Na_2O, K_2O, P_2O_5) and 28 trace elements were measured.

The concentrations of rare earth elements (REE) and other trace elements (Ba, Co, Cr, Cs, Cu, Ga, Hf, Nb, Ni, Pb, Rb, Sc, Sr, Ta, Th, U, V, W, Y, Zn, Zr) were determined by ICP-MS. One hundred milligrams of powder were dissolved in 5.0 ml HNO_3 (65%, doubly distilled) and 2.0 ml HF (40%) and heated for 12 h to 170 °C under pressure in Teflon bombs. After slowly cooling and the addition of 2.0 ml HNO_3 the solutions were nearly completely evaporated. Then 1.0 ml HNO_3 and 1.0 ml HCl were added, diluted with 20–30 ml H_2O and heated again to 170 °C. After cooling, the solution was refilled with doubly distilled water up to 100.0 g, and spiked with Rh and Re.

Sm–Nd isotopic analyses of seven selected dolerites and one camptonite were performed at the Mineralogical-Geological Museum, the University of Oslo. The Sm and Nd contents of the whole rocks were determined by isotope dilution. The analysis procedure has been described in detail by Mearns (1986). Sm and Nd were measured with a VG 354 multi-collector mass spectrometer. Nd isotope compositions were normalized to $^{146}Nd/^{147}Nd = 0.7219$. Results are shown in Table 4. Twelve analyses of the La Jolla Nd standard gave $^{143}Nd/^{144}Nd = 0.511864 \pm 13$ (2σ).

Major- and trace-element chemistry

The Scania dolerites range from basalts to basaltic andesites in the TAS (total alkalis v. silica) classification diagram (Fig. 4). One dyke, near Oderljunga (Sk 82), deviates and plots in the andesite field. The alkaline mafic dykes are classified as tephrites and basanites. The trachytic intrusions vary from tephrites to trachytes.

The majority of the dolerite samples are quartz-normative and have rather evolved compositions with Mg numbers between 55 and 30 (Fig. 5) indicating that the parental magmas are unlikely to represent primary mantle melts. The range of variation of major and selected trace elements is shown in Figure 5. The abundances

Table 2. *Concentrations of major (wt%) and trace elements (ppm) in dolerite dykes from Scania (Sk 1–Sk 150) and dolerite sills in Västergötland (Vg 153–Vg 159). The sample localities are given in Table 3. (normal type, XRF; italic – ICP-MS).*

Sample	Sk 1	Sk 20	Sk 26	Sk 29	Sk 36	Sk 38	Sk 41	Sk 46	Sk 48	Sk 50	Sk 51	Sk 60	Sk 70	Sk 82
Group	I	I	I	I	II	II	I	I	I	I	I	I	I	II
Mg#	38.76	43.73	50.79	52.97	32.20	32.40	35.66	50.61	43.02	52.80	38.48	47.69	42.15	32.06
SiO_2	47.06	48.70	49.23	48.85	51.88	50.78	47.67	47.57	47.52	47.97	48.74	47.30	47.17	55.86
TiO_2	3.63	2.95	2.09	2.02	2.76	2.79	3.84	2.43	2.99	2.27	2.94	2.65	3.12	1.83
Al_2O_3	12.86	12.67	14.20	14.37	12.75	12.59	12.64	13.92	13.08	14.17	12.81	13.51	13.23	14.43
Fe_2O_3*	16.02	15.24	12.53	12.08	13.93	14.13	16.65	13.26	14.87	12.78	14.66	13.77	14.65	10.24
MnO	0.20	0.21	0.18	0.17	0.19	0.21	0.22	0.17	0.19	0.18	0.20	0.18	0.18	0.16
MgO	5.12	5.98	6.53	6.87	3.34	3.42	4.66	6.86	5.67	7.22	4.63	6.34	5.39	2.44
CaO	9.00	8.14	10.16	10.36	7.28	7.38	8.47	10.53	9.44	10.51	8.77	10.31	9.20	5.50
Na_2O	2.35	2.62	2.18	2.23	2.68	2.71	2.49	1.94	2.25	1.98	2.30	1.97	2.36	3.29
K_2O	0.84	1.04	0.57	0.50	1.52	1.45	0.85	0.35	0.57	0.49	0.73	0.35	0.69	1.90
P_2O_5	0.42	0.30	0.20	0.19	0.56	0.54	0.47	0.22	0.31	0.19	0.73	0.28	0.33	0.65
LOI	1.93	1.69	1.49	1.71	1.87	2.99	1.40	2.02	2.53	1.67	2.65	2.65	2.95	2.97
Total	99.43	99.54	99.36	99.35	98.76	98.99	99.36	99.26	99.42	99.42	99.16	99.31	99.26	99.27
Ba	*263*	*378*	*867*	*485*	*537*	*539*	*342*	*108*	*209*	*376*	*310*	*137*	*212*	*568*
Co	*67.4*	*55.0*	*58.4*	*54.8*	*42.4*	*50.9*	*57.9*	*55.4*	*57.4*	*55.8*	*45.8*	*53.6*	*58.5*	*26.8*
Cr	*71.9*	*111*	*189*	*233*	*13.0*	*6.45*	*4.33*	*191*	*99.6*	*179*	*52.4*	*173*	*111*	*29.6*
Cs	*0.92*	*0.80*	*0.64*	*1.85*	*0.70*	*0.82*	*0.85*	*0.60*	*0.57*	*0.60*	*0.60*	*0.64*	*0.57*	*0.79*
Cu	*233*	*228*	*150*	*137*	*41.4*	*45.2*	*44.7*	*158*	*194*	*154*	*92.8*	*131*	*222*	*26.5*
Ga	*22.7*	*21.2*	*18.9*	*18.3*	*22.4*	*21.9*	*23.7*	*19.6*	*21.1*	*19.2*	*23.3*	*20.0*	*22.4*	*26.0*
Hf	*6.89*	*5.67*	*3.92*	*3.58*	*7.96*	*7.68*	*6.34*	*3.65*	*5.35*	*3.43*	*6.27*	*3.77*	*5.85*	*9.71*
Nb	*28.0*	*21.6*	*14.4*	*13.4*	*24.8*	*24.5*	*25.9*	*15.0*	*21.0*	*13.7*	*20.0*	*16.1*	*25.1*	*31.5*
Ni	*70.2*	*76.7*	*93.7*	*103*	*16.9*	*20.4*	*23.0*	*118*	*85.2*	*123*	*43.3*	*103*	*95.5*	*17.1*
Pb	*5.99*	*5.02*	*2.24*	*1.87*	*7.36*	*7.03*	*3.57*	*1.92*	*3.03*	*1.69*	*3.11*	*2.01*	*3.17*	*5.40*
Rb	*26.6*	*44.2*	*15.8*	*17.4*	*41.3*	*41.7*	*22.1*	*8.82*	*14.6*	*13.4*	*18.5*	*9.89*	*18.9*	*56.8*
Sc	*29.0*	*32.4*	*31.3*	*30.8*	*26.9*	*27.5*	*29.7*	*28.6*	*29.1*	*28.8*	*30.2*	*28.5*	*27.8*	*15.6*
Sr	*357*	*352*	*316*	*302*	*355*	*372*	*423*	*321*	*342*	*327*	*411*	*328*	*345*	*433*
Ta	*2.03*	*1.43*	*1.02*	*0.95*	*1.50*	*1.49*	*1.70*	*1.04*	*1.43*	*0.95*	*1.33*	*1.10*	*1.71*	*2.24*
Th	*2.86*	*2.14*	*1.54*	*1.39*	*5.01*	*4.78*	*2.48*	*1.27*	*2.08*	*1.20*	*2.25*	*1.29*	*2.62*	*6.62*
U	*0.63*	*0.48*	*0.34*	*0.32*	*0.90*	*0.86*	*0.59*	*0.30*	*0.48*	*0.28*	*0.47*	*0.31*	*0.61*	*1.40*
V	*412*	*431*	*326*	*314*	*291*	*302*	*428*	*335*	*369*	*317*	*334*	*356*	*358*	*149*
W	*166*	*93.3*	*126*	*89.6*	*55.5*	*123*	*91.4*	*75.4*	*88.0*	*76.7*	*68.0*	*62.8*	*110*	*62.9*
Y	*36.7*	*36.1*	*25.4*	*23.4*	*47.8*	*46.4*	*40.1*	*22.4*	*30.7*	*21.6*	*44.1*	*23.9*	*33.3*	*48.4*
Zn	*146*	*141*	*117*	*105*	*148*	*146*	*156*	*102*	*126*	*100*	*147*	*108*	*128*	*134*
Zr	*278*	*228*	*155*	*141*	*329*	*317*	*258*	*142*	*216*	*135*	*259*	*149*	*239*	*401*
La	*24.3*	*17.9*	*12.1*	*11.1*	*37.4*	*36.5*	*23.5*	*11.9*	*18.8*	*11.1*	*24.3*	*12.8*	*21.8*	*45.5*
Ce	*62.6*	*46.3*	*31.2*	*28.3*	*89.1*	*88.2*	*60.7*	*31.3*	*48.5*	*28.6*	*62.5*	*33.6*	*55.1*	*109*
Pr	*8.71*	*6.40*	*4.45*	*4.12*	*11.40*	*11.00*	*8.02*	*4.41*	*6.56*	*4.06*	*8.60*	*4.78*	*7.40*	*13.30*
Nd	*38.8*	*28.9*	*20.3*	*18.8*	*47.9*	*46.1*	*36.2*	*20.3*	*29.2*	*18.7*	*39.5*	*22.1*	*32.8*	*55.3*
Sm	*8.92*	*7.20*	*5.09*	*4.79*	*10.50*	*10.20*	*8.85*	*5.02*	*7.05*	*4.70*	*9.60*	*5.43*	*7.69*	*12.00*
Eu	*2.83*	*2.31*	*1.77*	*1.65*	*3.13*	*2.99*	*2.89*	*1.65*	*2.27*	*1.61*	*3.45*	*1.84*	*2.39*	*3.64*
Gd	*9.39*	*8.03*	*5.62*	*5.25*	*11.10*	*10.70*	*9.60*	*5.46*	*7.46*	*5.21*	*10.70*	*5.91*	*8.19*	*12.10*
Tb	*1.39*	*1.24*	*0.88*	*0.81*	*1.64*	*1.58*	*1.45*	*0.82*	*1.12*	*0.80*	*1.57*	*0.88*	*1.22*	*1.78*
Dy	*7.62*	*7.26*	*5.11*	*4.82*	*9.38*	*9.02*	*8.17*	*4.61*	*6.36*	*4.43*	*8.86*	*4.94*	*6.89*	*9.82*
Ho	*1.44*	*1.39*	*0.98*	*0.91*	*1.82*	*1.73*	*1.54*	*0.87*	*1.20*	*0.83*	*1.68*	*0.93*	*1.28*	*1.83*
Er	*3.81*	*3.78*	*2.66*	*2.44*	*4.97*	*4.77*	*4.14*	*2.28*	*3.16*	*2.23*	*4.51*	*2.45*	*3.40*	*4.96*
Tm	*0.49*	*0.50*	*0.35*	*0.34*	*0.67*	*0.65*	*0.54*	*0.30*	*0.41*	*0.29*	*0.57*	*0.32*	*0.45*	*0.65*
Yb	*3.05*	*3.12*	*2.18*	*2.01*	*4.10*	*3.97*	*3.30*	*1.85*	*2.53*	*1.75*	*3.57*	*1.96*	*2.75*	*4.01*
Lu	*0.47*	*0.48*	*0.34*	*0.32*	*0.65*	*0.63*	*0.50*	*0.28*	*0.38*	*0.27*	*0.55*	*0.30*	*0.43*	*0.62*

Sample	Sk 89	Sk 90	Sk 92	Sk 94	Sk 95	Sk 98	Sk 99	Sk 104	Sk 108	Sk 110	Sk 112	Sk 113	Sk 127	Sk 128
Group	II	II	I	II	II	II	I	I	II	I	I	I	II	I
Mg#	39.28	40.42	44.90	47.97	49.23	38.13	38.46	44.16	32.60	36.00	41.75	34.81	40.74	38.70
SiO_2	51.97	51.69	47.54	48.49	48.71	50.63	49.87	48.40	50.36	47.77	46.91	47.91	48.59	47.55
TiO_2	2.59	2.34	3.06	2.31	2.07	2.74	2.95	3.00	3.05	3.63	3.89	3.90	2.84	3.20
Al_2O_3	13.46	13.52	13.41	15.28	16.58	13.70	13.46	13.33	12.97	12.60	12.72	12.69	13.98	12.62
Fe_2O_3*	13.47	13.78	14.63	12.80	11.48	14.43	15.02	14.50	14.66	16.69	15.86	17.10	14.66	16.47
MnO	0.30	0.18	0.19	0.18	0.16	0.18	0.20	0.20	0.16	0.21	0.20	0.23	0.19	0.21
MgO	4.40	4.72	6.02	5.96	5.62	4.49	4.74	5.79	3.58	4.74	5.74	4.61	5.09	5.25
CaO	6.74	7.12	10.01	9.23	9.44	8.19	7.92	9.70	7.20	8.66	9.52	8.47	8.25	8.97
Na_2O	3.11	3.22	2.23	2.80	2.85	2.66	2.67	2.21	2.61	2.52	2.21	2.72	2.89	2.18
K_2O	1.26	1.26	0.55	0.80	0.73	0.99	1.14	0.60	1.32	0.79	0.83	0.85	0.78	0.62
P_2O_5	0.40	0.32	0.31	0.31	0.28	0.39	0.38	0.30	0.72	0.39	0.38	0.48	0.34	0.32

Table 2. *Continued.*

Sample	Sk 89	Sk 90	Sk 92	Sk 94	Sk 95	Sk 98	Sk 99	Sk 104	Sk 108	Sk 110	Sk 112	Sk 113	Sk 127	Sk 128
Group	II	II	I	II	II	II	I	I	II	I	I	I	II	I
Mg#	39.28	40.42	44.90	47.97	49.23	38.13	38.46	44.16	32.60	36.00	41.75	34.81	40.74	38.70
LOI	1.79	1.29	1.33	1.19	1.47	1.00	1.16	1.35	2.48	1.26	1.26	0.59	1.86	1.92
Total	99.49	99.45	99.29	99.34	99.38	99.41	99.50	99.38	99.10	99.26	99.52	99.55	99.46	99.30
Ba	*437*	*419*	*159*	*342*	*319*	*402*	*368*	*504*	*449*	*233*	*206*	*246*	*306*	*195*
Co	*50.5*	*52.6*	*55.5*	*52.3*	*51.1*	*53.5*	*53.9*	*59.4*	*50.4*	*61.1*	*54.6*	*57.8*	*54.5*	*56.7*
Cr	*18.4*	*24.0*	*147*	*158*	*157*	*21.9*	*35.2*	*81.5*	*6.73*	*6.89*	*138*	*5.79*	*62.7*	*32.3*
Cs	*0.51*	*0.32*	*0.29*	*0.64*	*0.67*	*0.60*	*0.48*	*0.50*	*0.58*	*0.97*	*0.74*	*0.59*	*0.24*	*0.58*
Cu	*132*	*134*	*229*	*183*	*164*	*29.1*	*41.8*	*194*	*63.4*	*114*	*287*	*47.8*	*154*	*41.4*
Ga	*23.2*	*22.2*	*20.4*	*20.6*	*21.2*	*23.1*	*22.9*	*22.5*	*23.0*	*24.0*	*22.5*	*24.2*	*23.0*	*22.8*
Hf	*8.99*	*6.83*	*5.24*	*5.78*	*5.18*	*6.95*	*5.42*	*5.50*	*7.84*	*6.26*	*6.33*	*6.45*	*7.26*	*4.65*
Nb	*31.4*	*21.5*	*18.2*	*21.0*	*18.9*	*25.2*	*21.2*	*20.8*	*26.1*	*24.4*	*21.9*	*25.1*	*26.6*	*18.2*
Ni	*64.7*	*51.4*	*83.7*	*154*	*163*	*30.5*	*35.2*	*77.0*	*19.0*	*41.1*	*85.9*	*22.8*	*95.0*	*34.6*
Pb	*8.41*	*7.05*	*2.85*	*4.06*	*3.75*	*5.54*	*4.78*	*2.61*	*6.69*	*3.47*	*3.01*	*3.51*	*5.21*	*3.43*
Rb	*42.2*	*42.3*	*16.3*	*22.0*	*19.2*	*28.0*	*40.2*	*17.2*	*41.3*	*24.3*	*40.6*	*26.3*	*24.7*	*17.4*
Sc	*26.2*	*29.8*	*33.2*	*26.4*	*24.9*	*27.1*	*27.6*	*32.1*	*29.6*	*31.5*	*34.0*	*30.8*	*29.2*	*30.0*
Sr	*343*	*355*	*318*	*367*	*411*	*415*	*391*	*339*	*314*	*384*	*343*	*402*	*361*	*346*
Ta	*1.85*	*1.33*	*1.24*	*1.32*	*1.19*	*1.62*	*1.39*	*1.55*	*1.70*	*1.71*	*1.54*	*1.76*	*1.67*	*1.22*
Th	*4.70*	*4.08*	*1.86*	*2.23*	*1.99*	*3.85*	*3.60*	*2.19*	*4.89*	*2.48*	*2.30*	*2.52*	*3.50*	*2.82*
U	*1.01*	*0.76*	*0.42*	*0.51*	*0.46*	*0.79*	*0.87*	*0.48*	*0.91*	*0.58*	*0.52*	*0.60*	*0.88*	*0.70*
V	*303*	*340*	*404*	*327*	*303*	*346*	*337*	*364*	*276*	*450*	*456*	*401*	*334*	*388*
W	*95.0*	*79.4*	*106*	*72.0*	*71.3*	*104*	*95.7*	*86.3*	*80.7*	*89.9*	*74.7*	*90.6*	*59.9*	*66.2*
Y	*47.7*	*40.4*	*32.9*	*34.1*	*30.3*	*36.3*	*32.8*	*32.0*	*49.2*	*38.1*	*38.7*	*39.0*	*41.4*	*28.9*
Zn	*145*	*137*	*115*	*118*	*107*	*157*	*134*	*131*	*157*	*151*	*132*	*148*	*132*	*133*
Zr	*374*	*278*	*206*	*240*	*216*	*286*	*216*	*216*	*312*	*244*	*247*	*250*	*291*	*177*
La	*35.9*	*28.3*	*16.4*	*23.1*	*20.4*	*31.5*	*22.9*	*18.8*	*37.4*	*22.8*	*19.8*	*23.0*	*28.0*	*19.2*
Ce	*86.5*	*68.5*	*42.2*	*55.5*	*50.0*	*74.6*	*56.7*	*47.0*	*88.2*	*56.1*	*49.5*	*57.7*	*66.8*	*45.6*
Pr	*10.70*	*8.47*	*5.97*	*7.26*	*6.48*	*9.40*	*7.20*	*6.56*	*11.40*	*7.70*	*7.07*	*7.83*	*8.66*	*6.05*
Nd	*45.8*	*35.9*	*27.5*	*31.0*	*27.9*	*39.6*	*31.4*	*29.6*	*48.6*	*34.8*	*32.8*	*35.6*	*37.7*	*26.8*
Sm	*10.40*	*8.24*	*6.89*	*7.13*	*6.46*	*8.60*	*7.35*	*7.25*	*11.00*	*8.47*	*8.32*	*8.72*	*8.78*	*6.48*
Eu	*2.99*	*2.43*	*2.23*	*2.26*	*2.08*	*2.67*	*2.57*	*2.39*	*3.28*	*2.75*	*2.66*	*2.85*	*2.67*	*2.32*
Gd	*10.90*	*8.88*	*7.66*	*7.73*	*6.89*	*8.98*	*7.90*	*7.76*	*11.70*	*9.27*	*9.16*	*9.57*	*9.58*	*6.98*
Tb	*1.65*	*1.36*	*1.16*	*1.17*	*1.04*	*1.32*	*1.18*	*1.16*	*1.73*	*1.39*	*1.38*	*1.42*	*1.45*	*1.05*
Dy	*9.36*	*7.79*	*6.70*	*6.65*	*5.90*	*7.29*	*6.66*	*6.60*	*9.91*	*7.87*	*7.95*	*8.20*	*8.32*	*5.86*
Ho	*1.81*	*1.53*	*1.27*	*1.29*	*1.16*	*1.39*	*1.24*	*1.24*	*1.91*	*1.47*	*1.52*	*1.52*	*1.60*	*1.11*
Er	*5.00*	*4.19*	*3.41*	*3.55*	*3.12*	*3.72*	*3.31*	*3.34*	*5.24*	*3.94*	*4.10*	*4.07*	*4.37*	*2.96*
Tm	*0.67*	*0.57*	*0.46*	*0.47*	*0.43*	*0.50*	*0.44*	*0.44*	*0.71*	*0.52*	*0.54*	*0.53*	*0.59*	*0.39*
Yb	*4.14*	*3.54*	*2.85*	*2.94*	*2.66*	*3.10*	*2.68*	*2.68*	*4.45*	*3.09*	*3.38*	*3.26*	*3.64*	*2.36*
Lu	*0.65*	*0.56*	*0.43*	*0.47*	*0.42*	*0.48*	*0.42*	*0.42*	*0.71*	*0.49*	*0.52*	*0.50*	*0.57*	*0.38*

Sample	Sk 130	Sk 132	Sk 133	Sk 134	Sk 145	Sk 146	Sk 150	Vg 153	Vg 154	Vg 155	Vg 156	Vg 158	Vg 159
Group	I	II	I	I	I	II	I						
Mg#	39.84	45.23	46.14	42.52	38.30	33.99	35.39	46.66	48.75	50.02	49.09	42.47	43.04
SiO_2	47.23	50.38	48.35	47.87	49.59	51.88	48.54	49.15	49.28	48.91	49.07	50.56	50.10
TiO_2	3.62	2.12	2.72	2.91	3.11	2.75	3.47	1.97	1.95	1.96	1.95	2.23	2.19
Al_2O_3	13.11	14.44	13.85	13.54	13.35	13.04	13.06	14.65	14.65	14.65	14.69	14.03	14.05
Fe_2O_3*	15.79	12.88	13.87	12.37	15.22	14.19	14.75	13.20	13.16	13.32	13.31	14.11	14.05
MnO	0.20	0.17	0.18	0.24	0.21	0.16	0.23	0.20	0.18	0.18	0.18	0.17	0.18
MgO	5.28	5.37	6.00	4.62	4.77	3.69	4.08	5.83	6.32	6.73	6.48	5.26	5.36
CaO	9.33	8.84	9.33	10.76	7.37	5.77	7.77	9.70	9.67	9.85	9.70	8.68	8.77
Na_2O	2.35	2.77	2.13	2.21	2.54	2.72	3.75	2.60	2.65	2.54	2.48	2.82	2.77
K_2O	0.62	0.89	0.47	0.55	1.39	1.96	0.48	0.48	0.48	0.44	0.45	0.89	0.82
P_2O_5	0.79	0.30	0.27	0.29	0.39	0.63	1.31	0.20	0.20	0.19	0.21	0.33	0.32
LOI	1.20	1.29	1.98	4.06	1.61	2.54	1.90	1.47	0.98	0.79	1.03	0.40	0.75
Total	99.53	99.45	99.15	99.41	99.54	99.32	99.34	99.45	99.51	99.55	99.54	99.48	99.35
Ba	*208*	*319*	*328*	*594*	*535*	*680*	*345*	*183*	*190*	*166*	*177*	*369*	*339*
Co	*53.3*	*58.5*	*56.8*	*51.6*	*55.2*	*45.7*	*39.1*	*58.6*	*63.2*	*72.8*	*60.3*	*67.3*	*59.0*
Cr	*73.0*	*58.9*	*116*	*102*	*29.2*	*8.43*	*6.80*	*55.4*	*55.0*	*65.1*	*56.9*	*43.5*	*45.8*
Cs	*0.59*	*0.52*	*0.57*	*0.44*	*0.65*	*0.95*	*0.47*	*1.00*	*0.36*	*0.66*	*0.49*	*0.71*	*0.89*
Cu	*84.8*	*147*	*180*	*190*	*42.1*	*56.2*	*24.3*	*88.9*	*90.2*	*105*	*101*	*61.5*	*65.6*
Ga	*22.8*	*20.9*	*22.1*	*22.1*	*23.2*	*22.6*	*24.1*	*20.8*	*21.3*	*20.3*	*20.3*	*22.1*	*22.0*
Hf	*5.23*	*5.97*	*4.95*	*5.15*	*5.51*	*8.31*	*7.33*	*3.70*	*3.73*	*3.53*	*3.38*	*5.44*	*5.28*
Nb	*22.4*	*21.9*	*18.0*	*19.4*	*21.2*	*25.8*	*27.5*	*11.3*	*11.0*	*10.9*	*11.0*	*13.0*	*12.5*
Ni	*53.4*	*84.6*	*99.9*	*86.4*	*32.8*	*17.3*	*14.8*	*68.2*	*70.5*	*87.2*	*77.3*	*49.2*	*53.2*
Pb	*3.71*	*4.92*	*4.52*	*2.97*	*3.94*	*7.37*	*4.11*	*2.44*	*2.55*	*2.35*	*2.26*	*4.83*	*4.76*

Table 2. *Continued.*

Sample	Sk 130	Sk 132	Sk 133	Sk 134	Sk 145	Sk 146	Sk 150	Vg 153	Vg 154	Vg 155	Vg 156	Vg 158	Vg 159
Group	I	II	I	I	I	II	I						
Mg#	39.84	45.23	46.14	42.52	38.30	33.99	35.39	46.66	48.75	50.02	49.09	42.47	43.04
Rb	19.2	26.6	12.6	13.2	55.3	61.6	14.3	10.7	10.8	10.2	10.5	26.8	23.7
Sc	26.9	28.8	31.7	31.3	27.9	27.6	26.5	30.2	31.0	30.6	29.8	28.9	28.8
Sr	370	355	322	346	382	321	509	343	404	354	360	454	491
Ta	1.60	1.38	1.30	1.37	1.45	1.72	1.94	0.78	0.78	0.78	0.78	0.89	0.88
Th	2.27	2.70	1.81	2.03	3.65	5.44	2.95	1.41	1.39	1.29	1.31	3.14	2.95
U	0.49	0.61	0.42	0.46	0.87	1.00	0.64	0.29	0.28	0.27	0.27	0.49	0.47
V	354	304	334	338	328	232	213	284	279	283	273	293	286
W	85.9	134	63.3	44.9	84.6	71.2	49.9	77.1	110	166	98.0	156	95.5
Y	34.7	34.5	28.4	30.2	32.4	49.7	47.8	25.2	25.4	24.4	25.0	31.4	30.9
Zn	138	114	118	117	137	104	143	99.4	105	101	103	118	116
Zr	202	243	188	198	211	323	288	140	138	129	122	207	200
La	23.9	25.2	16.8	18.5	22.1	37.0	40.7	13.9	13.9	12.3	13.3	26.8	25.2
Ce	58.7	57.5	41.1	44.4	54.2	87.3	97.6	32.2	31.9	29.1	31.1	59.8	56.0
Pr	7.96	7.41	5.81	6.30	7.10	11.30	13.10	4.50	4.40	4.09	4.37	7.83	7.42
Nd	36.2	31.5	26.2	28.4	30.9	47.9	58.6	20.3	19.9	18.7	19.7	33.2	31.6
Sm	8.54	7.13	6.41	6.94	7.30	10.80	13.00	5.06	5.00	4.81	4.95	7.24	6.99
Eu	2.75	2.17	2.12	2.37	2.59	3.25	4.32	1.79	1.76	1.73	1.79	2.23	2.18
Gd	9.04	7.72	6.91	7.52	7.96	11.60	13.50	5.73	5.61	5.43	5.66	7.69	7.43
Tb	1.32	1.17	1.05	1.11	1.18	1.73	1.86	0.89	0.88	0.85	0.89	1.14	1.12
Dy	7.09	6.80	5.90	6.26	6.60	9.81	10.00	5.19	5.04	5.00	5.02	6.45	6.26
Ho	1.33	1.32	1.11	1.19	1.26	1.91	1.85	1.00	0.97	0.95	0.99	1.24	1.20
Er	3.53	3.65	3.02	3.13	3.31	5.33	4.88	2.75	2.69	2.61	2.63	3.39	3.31
Tm	0.45	0.50	0.40	0.42	0.44	0.71	0.61	0.37	0.36	0.35	0.36	0.45	0.44
Yb	2.71	3.11	2.42	2.49	2.66	4.42	3.69	2.21	2.22	2.12	2.16	2.77	2.67
Lu	0.42	0.50	0.38	0.40	0.43	0.70	0.57	0.35	0.34	0.34	0.33	0.43	0.42

[1] LOI, loss on ignition; [2] $Fe_2O_3^*$ as total iron; [3] Mg#, Mg number.

of SiO_2, TiO_2, $Fe_2O_3^*$, Na_2O, K_2O and P_2O_5 increase with decreasing Mg number, while the concentration of Al_2O_3 and CaO decrease. Trace elements behave similarly; concentrations of Ni and Cr decrease, but those of Ba, Nb, Rb, Th and Zr increase. Sr contents are nearly constant.

The Mg-numbers of the alkaline mafic rocks range from 65 to 40 (Fig. 5). Although these values are mostly higher than those of the dolerites, these rocks generally cannot be considered as representatives of primary melts. Only two camptonite samples from Torpa Klint in central Scania and the alkali basalt from Nyhamnsläge in NW Scania have high Mg numbers and relatively high concentrations of Cr and Ni, but are still somewhat removed from primary melt compositions that could have been in equilibrium with mantle olivine. The rocks are all SiO_2 undersaturated and are enriched in large ion lithophile elements (LILE, e.g. K, Ba, Sr), P and volatiles (CO_2), which is typical of alkaline lamprophyres (Rock 1991). The group is geochemically heterogeneous as indicated by variable concentration of most elements. Rough decreasing trends are shown in the plots for Ni and Cr v. Mg number. Increasing trends for TiO_2 and Al_2O_3 are indicated only by the samples from central Scania; the samples of NW Scania deviate by their higher and lower values, respectively.

The alkaline mafic rocks can be easily separated from the dolerites by means of specific trace elements such as Ba, Nb, Sr and Th. Nb especially appears to be a useful discriminator and allows a complete separation of the two (Fig. 5). Furthermore, in contrast to the wide variation of Sr among the alkaline mafic rocks (500–2000 ppm), the dolerites show a much smaller range between 250 and 500 ppm. Most of the alkaline rocks contain more than 800 ppm Ba, while the dolerites have less than 600 ppm.

Two groups of dolerites (I and II) can be distinguished in a Zr–TiO_2 plot (Fig. 6). The dolerites I show steeper trends for TiO_2 and Fe_2O_3 v. Mg-number but a shallower trend for K_2O. Dolerites I and II define slightly different trends in the La–Sm diagram but cannot be discriminated in the La–Yb diagram. The dolerites of both groups also show moderate scatter in the ratios between highly incompatible elements such as La/Nb, but the samples of group II have much more variable Th/Ta ratios than group I. It has to be noted that these compositional differences are not limited to a certain area, nor to specific orientation or relative age of the dykes.

Table 3. *Sample localities of Scania dolerite dykes (Sk 1–Sk 150) and Västergötland dolerite sills (Vg 153–Vg 159)*

Sample	Locality	N	W	Sample	Locality	N	W
Sk 1	Hällestad	61726	13497	Sk 104	Röstånga	62095	13432
Sk 20	Tygelsjö	61761	13435	Sk 108	Kågeröd	62098	13315
Sk 26	Sularpsbäck	61790	13429	Sk 110	Eka Stiga	62058	13574
Sk 29	Skrylle	61767	13460	Sk 112	L. Svenstorp	62127	13544
Sk 36	Östraby	61821	13682	Sk 113	Smälteröd	62143	13506
Sk 38	Bjärsjölagård	61804	13700	Sk 127	Eket	62374	13370
Sk 41	Djurröd	61750	13833	Sk 128	Rävahallen	62411	13431
Sk 46	Ingelstad	61565	13905	Sk 130	Åslidehus	62390	13313
Sk 48	Bollerup	61528	13899	Sk 132	Röinge	62269	13758
Sk 50	Ingelstad	61573	13916	Sk 133	Nyhamnsläge	62405	12969
Sk 51	Gårdlösa	61597	13940	Sk 134	Nyhamnsläge	62403	12970
Sk 60	Vilhelmsberg	61587	14039	Sk 145	Båstad	62589	13192
Sk 70	Örnahusen	61475	14022	Sk 146	Kågeröd	62106	13302
Sk 82	Oderljunga	62320	13475	Sk 150	Brantaberg	62197	13800
Sk 89	Rekeroken	62401	13056	Vg 153	Kinnekulle	65000	13505
Sk 90	Svanshall	62403	13054	Vg 154	Kinnekulle	65000	13505
Sk 92	Skäret	62412	13022	Vg 155	Kinnekulle	65000	13505
Sk 94	Arild	62437	12995	Vg 156	Kinnekulle	65000	13505
Sk 95	Arild	62436	12996	Vg 158	Hunneberg	64755	13755
Sk 98	Hallandsås	62506	13216	Vg 159	Hunneberg	64755	13755
Sk 99	Torekov	62612	13045				

Table 4. *Results of Sm–Nd isotope analyses of Scania dykes (D I/II, dolerite group I/group II; C, camptonite). K–Ar ages from Klingspor (1976). Major- and trace-element concentrations of these samples are published in Obst (1999)*

Sample		K–Ar age (Ma)	Sm (ppm)	Nd (ppm)	$^{143}Nd/^{144}Nd$ (measured)	2σ	$^{147}Sm/^{144}Nd$ (± 0.25%)	εNd (measured)	εNd (K–Ar)	εNd (300 Ma)
Sk 3	D I	291 ± 4	5.77	22.72	0.512770	± 8	0.154582	+2.40	+4.15	+4.02 ± 0.29
Sk 21	D I	295 ± 4	5.21	20.71	0.512738	± 8	0.153296	+1.78	+3.59	+2.80 ± 0.21
Sk 79	D II	287 ± 4	11.04	53.35	0.512480	± 10	0.126001	−3.25	−0.49	−0.55 ± 0.22
Sk 81	D II	293 ± 4	6.96	30.40	0.512516	± 10	0.139464	−2.55	−0.24	−0.36 ± 0.24
Sk 84	D I	312 ± 4	5.97	23.61	0.512736	± 8	0.154020	+1.74	+3.62	+3.37 ± 0.29
Sk 87	D II	297 ± 4	8.47	36.00	0.512471	± 6	0.143263	−3.43	−1.23	−1.39 ± 0.23
Sk 88	D II	318 ± 5	7.52	32.79	0.512521	± 12	0.139611	−2.46	+0.04	−0.27 ± 0.21
Sk 122	C	274 ± 4	7.60	47.45	0.512596	± 8	0.097569	−0.99	+2.65	+2.80 ± 0.21

Mantle-normalized incompatible element patterns emphasize geochemical variations within the dolerites. Apart from a very few, relatively less evolved, dykes of group I with MgO contents > 6% (subgroup Ia), which occur along the southern margin of the dyke swarm, all other studied dolerites show trace-element patterns with a marked trough at Sr (Fig. 7). The more primitive dolerites also have a distinct positive Nb–Ta peak and relatively low concentrations of Yb. A positive anomaly at Nb–Ta is also common for the more evolved dolerites of group I with MgO concentrations less than 6% (subgroup Ib). A few dolerites of group II, among the plagioclase-phyric types, have only a slight positive peak at Nb–Ta together with a negative anomaly at Ti (subgroup IIa). Other dolerites of this group have a trough at Nb–Ta combined with a trough at Ti (subgroup IIb). Exceptions that have deviating element patterns occur in both dolerite groups. Samples Sk 99 and Sk 145 have a slight positive peak at K. Sample Sk 150, taken from the chilled margin of a dyke near Branteberg, has a rather flat pattern like the less evolved dolerites of subgroup Ia, but seems to be relatively enriched in LREE and depleted in LILE. Samples Sk 89 and Sk 127 have a pattern similar to those from subgroup IIa, but are also characterized by higher concentrations of Ba, Th and U.

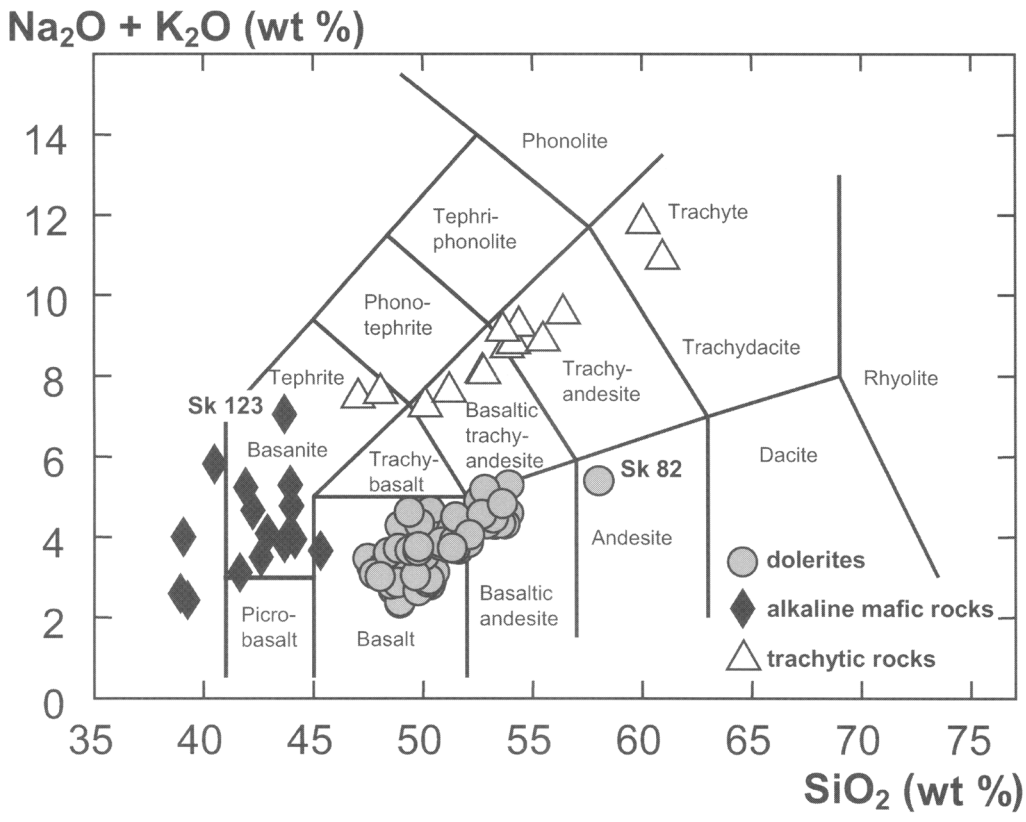

Fig. 4. Total alkalis v. SiO_2 classification diagram for volcanic rocks (Le Maitre 2002). The dolerites trend from basalts to basaltic andesites (sample Sk 82 has large amounts of K-feldspar–quartz intergrowths). The alkaline mafic rocks plot mainly in the field of tephrite and basanite (sample Sk 123 contains numerous felsic ocelli). The trachytic dykes define a linear trend from tephrites to trachytes. Data: this study and Obst (1999).

Isotope signatures

$\varepsilon Nd(t)$ values were calculated using K–Ar ages (T_1) determined by Klingspor (1976) for individual dykes, and for a theoretical age of 300 Ma (T_2) close to the Permo-Carboniferous border using the timescale of Menning *et al.* (2000). The Nd isotope data also reflect the existence of the two geochemically different dolerite groups. Dolerites I are characterized by positive εNd values at the time of intrusion between $+4$ and $+3$ reflecting a slightly depleted mantle source, while the dolerites II have values of about 0 to -1 (Fig. 8).

Discussion of the petrogenesis of the mafic dykes

The compositional data presented above imply that the dolerites and the alkaline mafic rocks of the Scania dyke swarm were generated from different sources and have been subsequently subjected to different processes – mixing, fractional crystallization and crustal contamination.

Crustal contamination and secondary alteration

Storage of mafic mantle melts in crustal magma chambers often leads to interaction and assimilation of the wall rocks (e.g. Peng *et al.* 1994). Major-element data can be used to assess the possibility of mixing with silicic crustal material. The group I dolerites clearly show no increase of SiO_2 concentration with decreasing Mg number (Fig. 9a), as typical of gabbro fractionation. The group II dolerites are characterized by an increasing trend, instead, which is possibly related to crustal contamination. Slight negative Nb–Ta troughs in trace-element patterns of the evolved group II dolerites compared to those of the evolved group I dolerites with positive peaks

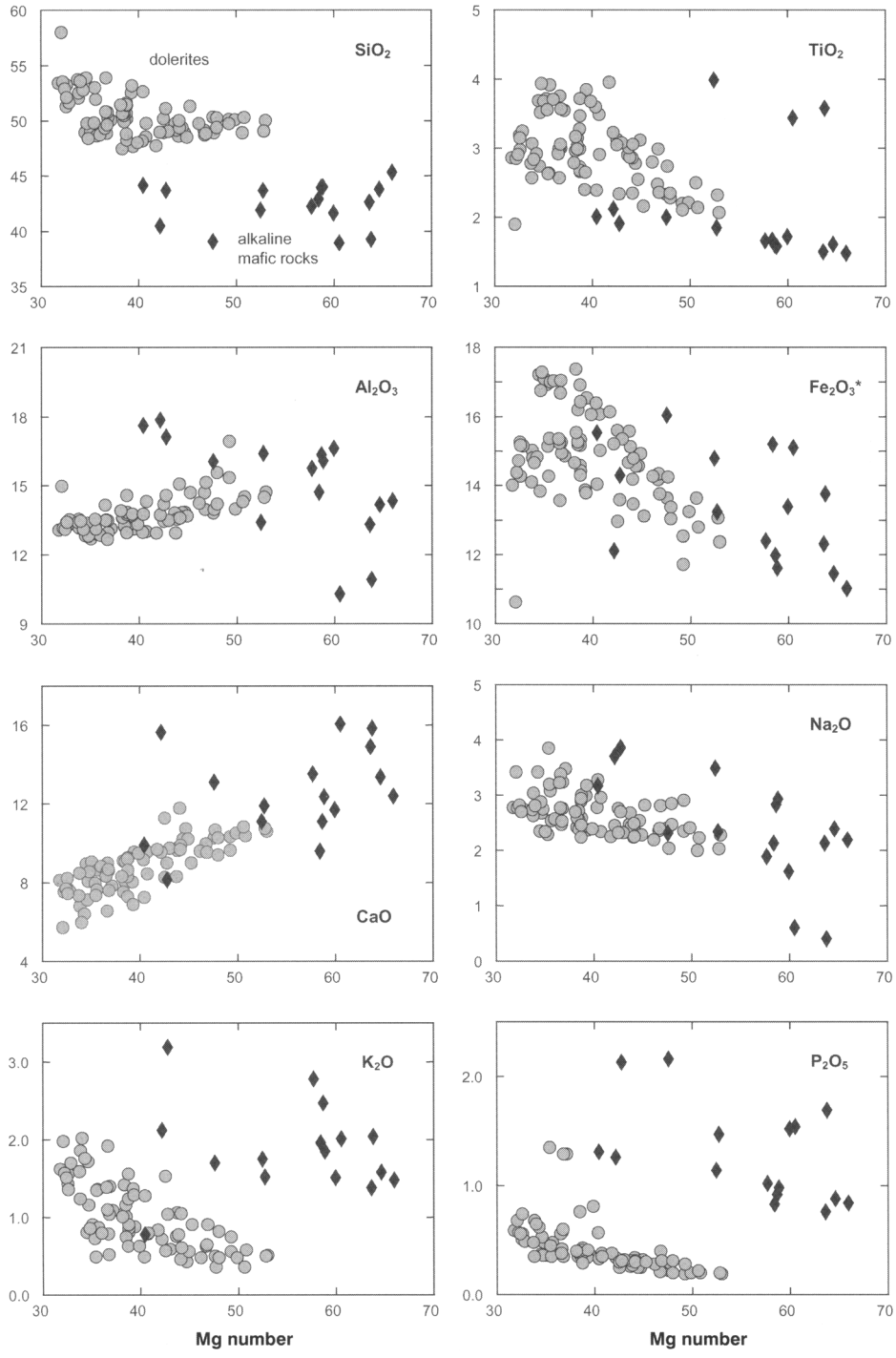

Fig. 5. Major- and trace-element variation diagrams v. Mg-number for the mafic dykes of Scania. The Mg-number is used as a differentiation index. The dolerites mostly show linear trends indicating crystal fractionation. The alkaline mafic rocks can be distinguished from the dolerites by higher concentrations of K, P, Nb, Sr and Ba. Major elements are shown as oxides in wt%, and trace elements in ppm.

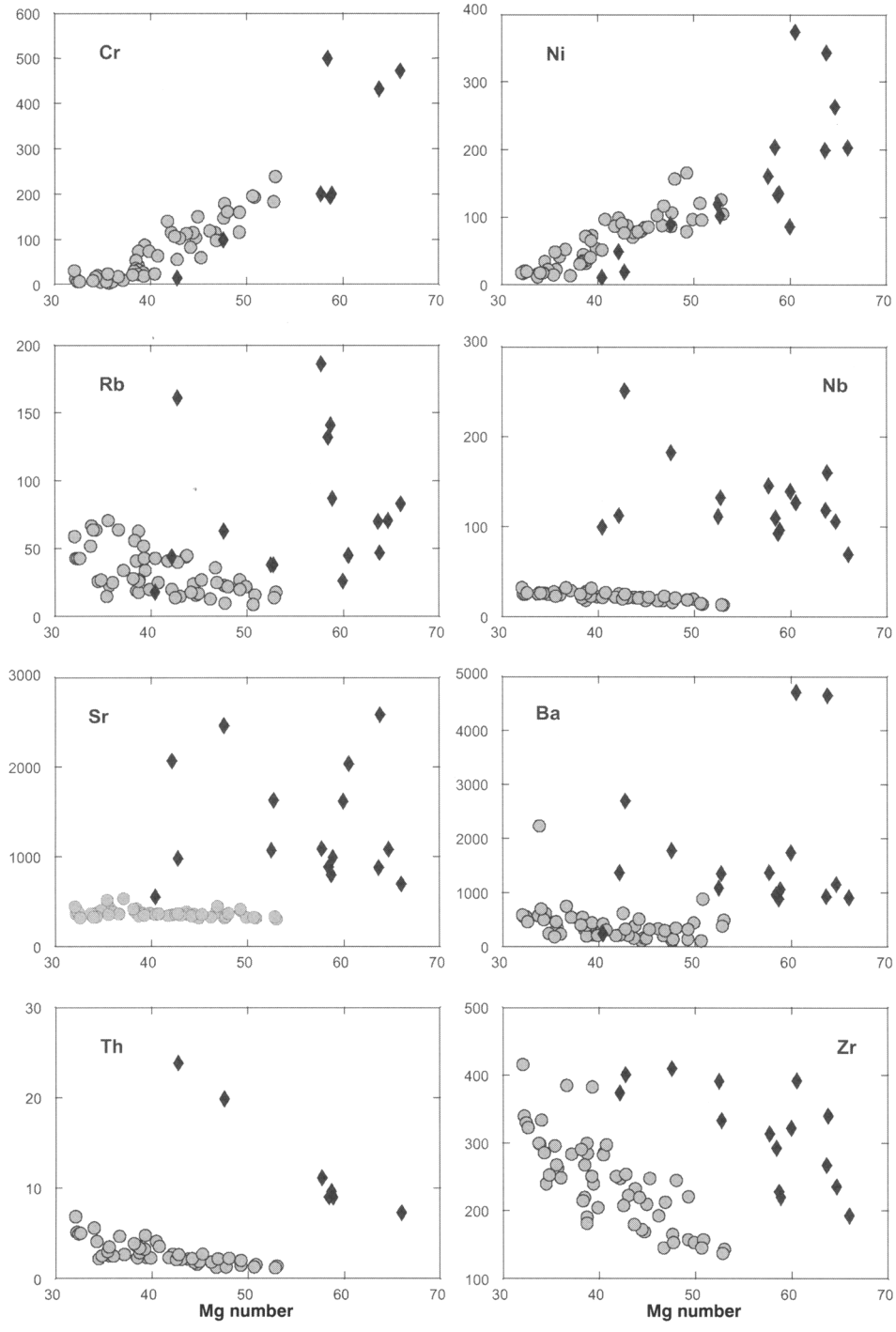

Fig. 5. Continued.

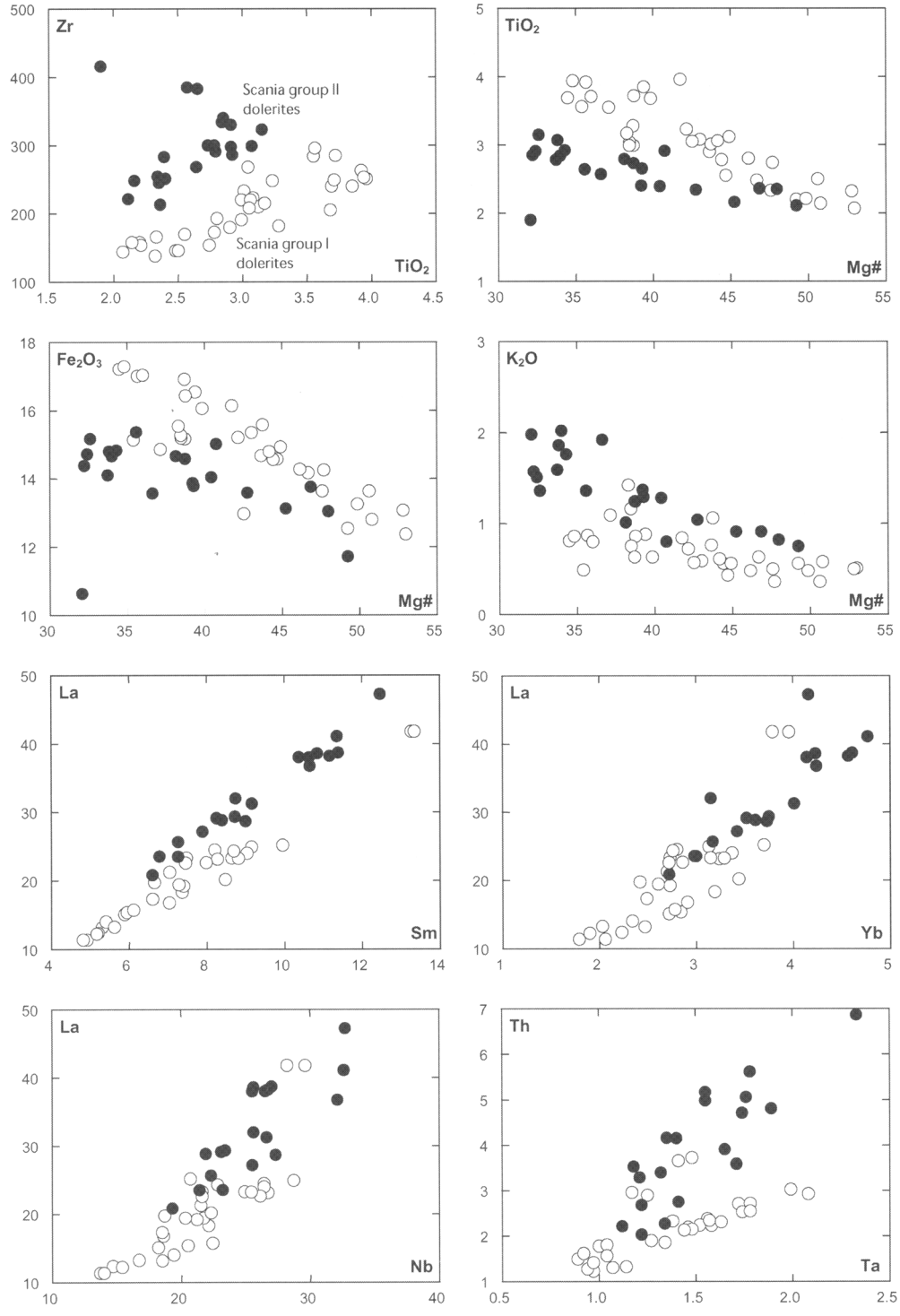

Fig. 6. Different trends in bivariate element plots indicating the existence of two dolerite groups (I, open circles; II, filled circles) in Scania.

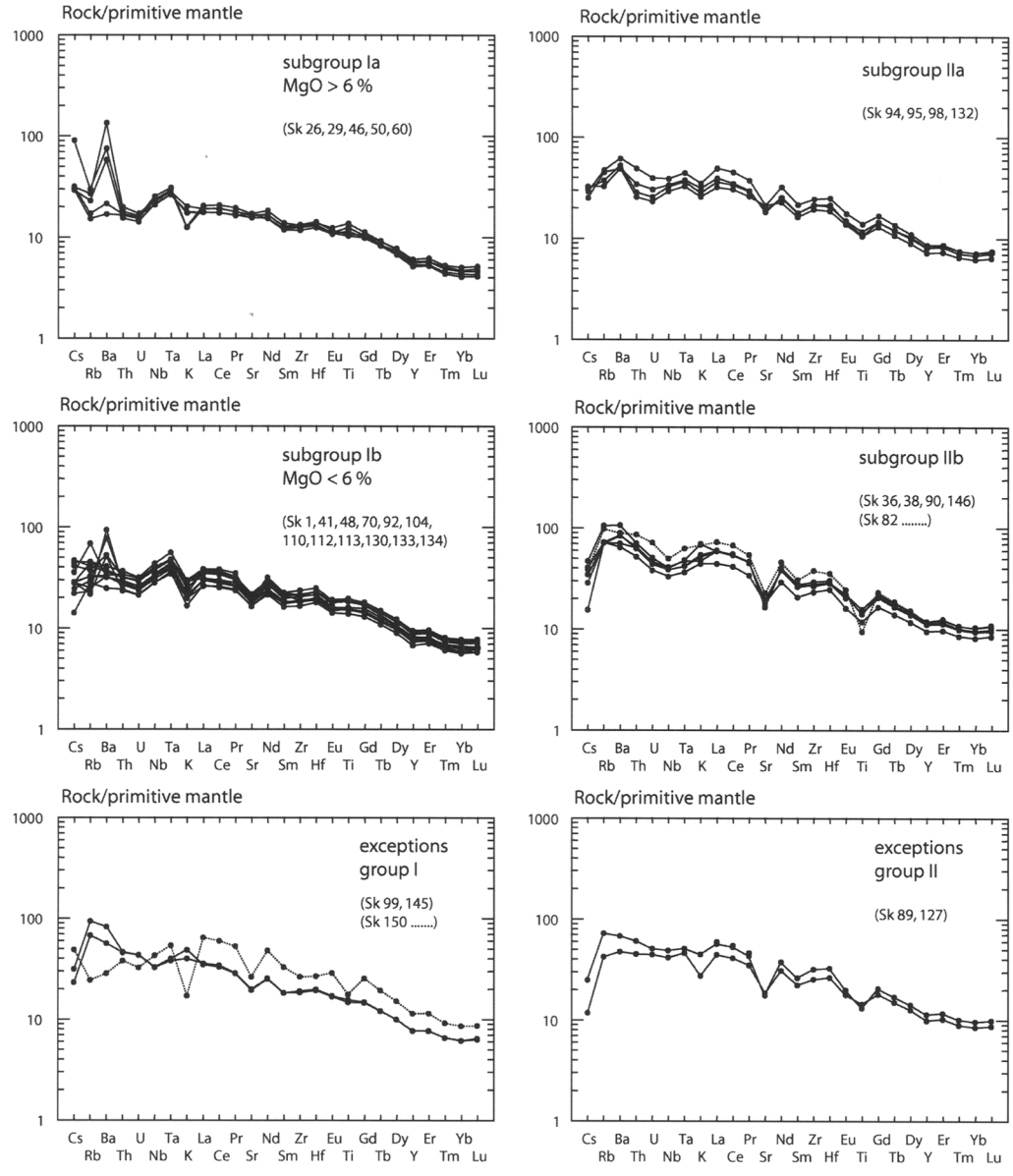

Fig. 7. Primitive mantle-normalized trace-element variation diagrams for the Scania dolerite dykes emphasizing the existence of two different dolerite groups (I, left; II, right). Apart from a few 'primitive' dykes (subgroup Ia), which show a positive or no Sr peak, the dolerites are mostly characterized by a negative trough at Sr. Most group I dolerites show a positive Nb–Ta anomaly, while the group II dolerites are often marked by a negative TNT (Ta–Nb–Ti) anomaly, except for a few less evolved dykes (subgroup IIa). Some samples have deviating patterns. Normalization factors are from McDonough & Sun (1995).

at Nb–Ta (see Fig. 7) additionally suggest a possible crustal influence.

In Figure 9b Nb/U concentrations of the dolerites are plotted v. the Th/Ta ratio. The Nb/U concentrations in uncontaminated basalts should be about 50 (Hofmann *et al.* 1986). Crustal rocks have significantly lower ratios. The group I dolerites have Nb/U ratios between and, while most of the group II dolerites have ratios <40. The samples seem to form a hyperbolic array, suggesting a mixing trend. The group II dolerites appear to be more

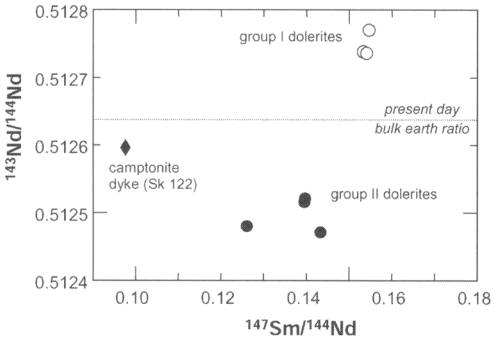

Fig. 8. $^{143}Nd/^{144}Nd$ v. $^{147}Sm/^{144}Nd$ diagram, illustrating the distinction between dolerite groups I and II. The group I dolerite samples have measured Nd isotope ratios typical of a moderately depleted mantle source. The dolerite II samples are characerized by lower Nd isotope ratios.

crustally contaminated, as their relatively high Th/Ta ratios indicate. A few dolerites classified as group I samples seem also to be crustally contaminated, for example the samples Sk 99 and Sk 145 both with the exceptional K peak in their trace-element patterns (see Fig. 7).

Furthermore, in a La/Sm v. La/Yb plot (Fig. 9c) the dolerite group II samples have higher La/Sm ratios than those of group I, which can also be related to crustal contamination. The initial Nd isotope ratios (εNd_i) are plotted against the K/Zr ratio, which compares a highly incompatible element and a less incompatible element (Fig. 9d). A correlation between this variable and an isotope ratio is indicative of a crustal contamination process. The sample distribution suggests that particularly the mantle-derived melts of dolerite group II were contaminated by small amounts of crustal material.

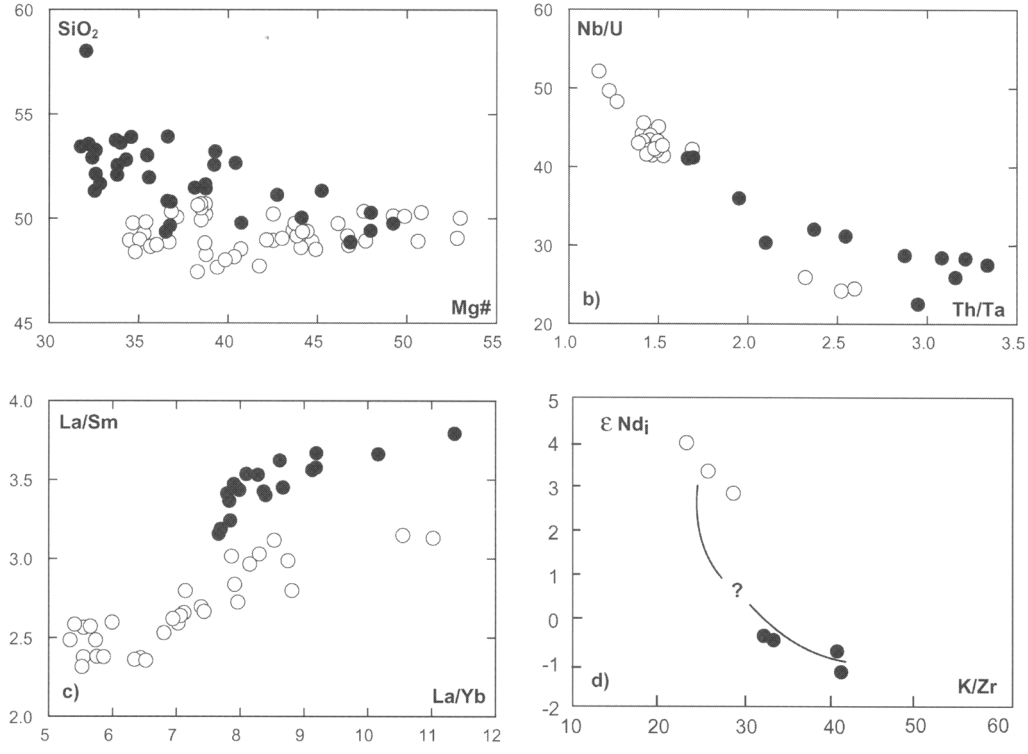

Fig. 9. (**a**) Variation of SiO_2 v. Mg-number (Mg#). Relatively constant SiO_2 concentrations in the Scania group I dolerites that correlate with decreasing Mg numbers is typical for a normal gabbro fractionation. The group II dolerites show an increasing trend that might result from crustal contamination. (**b**) Both dolerite groups have different Nb/U and Th/Ta ratios that decrease and increase from group I towards group II, respectively, forming a mixing hyperbola. This indicates increasing crustal influence. (**c**) The higher La/Sm ratios of group II dolerites may reflect crustal contamination but can also be due to differences in source composition for the two dolerite groups. (**d**) The initial εNd values (T = 300 Ma) plotted v. K/Zr suggest that group II dolerites, in particular, are crustally contaminated.

Crustal contamination or hybridization has also affected the alkaline mafic melts as suggested by the presence of trachytic schlieren of similar mineralogy to the silica-rich kullaites in some of the rocks. Calculated mixing trends support the assumption that the variable composition of the trachytic dykes is due to mixing of mantle-derived magmas with anatectic crustal melts of intermediate composition (Obst 1999).

Many of the investigated mafic rocks show changes in their primary mineral composition, especially the dolerite samples that have suffered from sericitization of plagioclase and chloritization of clinopyroxene. These post-magmatic alteration processes are also documented by scattering in the concentrations of the most incompatible and mobile elements, such as Ba and Rb (see Fig. 7).

Fractionation and magma sources

The dolerites consist mainly of plagioclase and clinopyroxene as described above. They mostly have MgO concentrations $< 6\%$ and trace-element patterns with a marked trough at Sr (see Fig. 7). This indicates that the parent melts have undergone fractional crystallization of ferromagnesian minerals and early fractionation of plagioclase at low pressure. Only the group I dolerites with MgO contents of $> 6\%$ represent less evolved melts and, thus, still contain pseudomorphs after olivine.

While the dolerites show enrichment in incompatible elements typical of continental tholeiites, the alkaline mafic rocks are even more enriched, and have higher LREE/HREE ratios and a much more pronounced negative K anomaly (Fig. 10a). This is a characteristic feature of alkaline melts generated either by very low degrees of partial melting of a garnet-bearing mantle source or from a veined mantle source (Foley 1992) indicating an early stage of magma production. The tholeiitic dolerites are probably generated from a different mantle source at a higher degree of partial melting; however, the sample distribution in several of the bivariate plots (see Fig. 6) suggests that this source is not homogenous, and allows us to subdivide the dolerites into two groups.

Subdivision of dolerite suites, reflecting the contribution of different mantle sources or the involvement of additional crustal components in their formation is not unusual for continental flood basalt (CFB) provinces. Their origin is under discussion. Some authors believe that the generation of CFBs is either related to the arrival of a plume head below the continental lithosphere or to lithospheric rifting and subsequent upwelling and melting of the hot asthenosphere (White & McKenzie 1989; Campbell & Griffiths 1990; Arndt & Christensen 1992; Anderson 1994). Thus, these magmatic provinces should be dominated by melts derived from the sublithospheric mantle. Heating by the

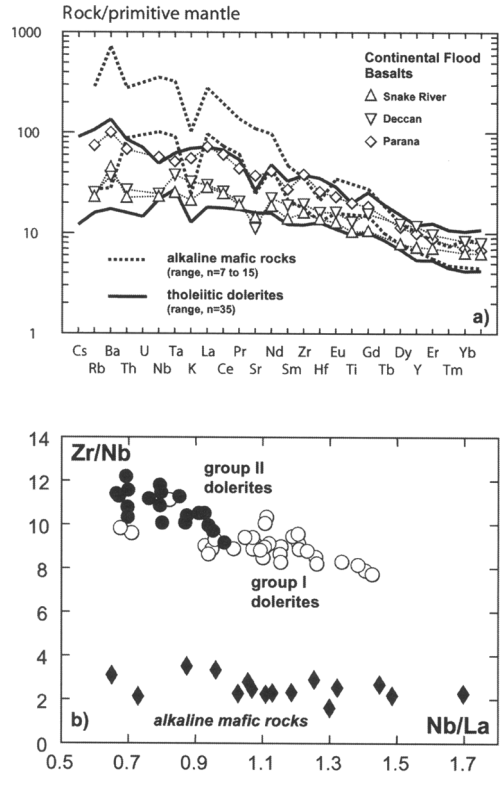

Fig. 10. (**a**) Mantle-normalized trace-element patterns for the mafic dykes of Scania compared to classic continental flood basalts (CFBs). The dolerites are enriched in LREE, as is typical for continental-type tholeiites (MgO-rich CFBs except the sample from the Paraná; data from Thompson *et al.* 1983). The pattern of the alkaline rocks is similar to those of alkaline melts generated from a metasomatized mantle source. Normalization factors are from McDonough & Sun (1995). (**b**) Zr/Nb v. Nb/La diagram. Group I dolerites mostly have Nb/La ratios > 0.9 typical of magmas derived from a sublithospheric mantle source, while the group II dolerites mostly have ratios < 0.9, interpreted as sign of melt generation from the continental lithospheric mantle. The slight increase of Zr/Nb with decreasing Nb/La in the group II samples might be due to crustal contamination. The Zr/Nb ratios of the alkaline mafic rocks are very different compared to the dolerites, and the varying Nb/La ratios suggest that they were generated not only from a different, but also from a heterogeneous, mantle source.

plume and rising magmas, however, may cause additional melting of the lithosphere. This is suggested by the observed trace-element ratios and isotope compositions of the most primitive mafic rocks, which are distinct from oceanic basalts. These magmas can be derived from incompatible-element-enriched source regions in the subcontinental lithospheric mantle, combined with crustal contamination (Hawkesworth *et al.* 1988; Hergt *et al.* 1991; Peng *et al.* 1994; Peate & Hawkesworth 1996).

Nearly all group I dolerites have a distinct positive Nb–Ta peak that may reflect generation from a sublithospheric mantle source (Arndt & Christensen 1992). The very low concentrations of Yb in the most primitive group I samples (subgroup I a), about 4–5 times higher than the concentration in primitive mantle, might indicate the existence of garnet in the magma source, either in the lherzolite itself or in garnet pyroxenite veins (Hirschmann & Stolper 1996).

The trace-element patterns of the group II dolerites are different from those of group I. A few less evolved samples, among the plagioclase-phyric types, have a slight positive peak at Nb–Ta together with a negative anomaly at Ti (subgroup IIa), while the other samples of this group have a trough at Nb–Ta combined with a trough at Ti (subgroup IIb), similar to, but not as strong as, that displayed by subduction-related magmas. This may reflect generation from a lithospheric mantle source enriched in LILE or crustal contamination as discussed above.

Differences in source composition between the dolerite groups itself and the alkaline mafic rocks are also detectable in the Zr/Nb v. Nb/La diagram (Fig. 10b). The dolerites have Zr/Nb ratios ranging from 7 to >12, while the alkaline mafic rocks are marked by lower and constant ratios of about 3. The dolerites show a wide range of Nb/La ratios, but the dolerites of group I particularly have ratios mostly >0.9, typical of OIB (Arndt & Christensen 1992), that could indicate generation of the primitive melts from an asthenospheric source, which is enriched in incompatible elements (plume head or metasomatic overprint?) suggested by the incompatible trace-element patterns. The group II dolerites mostly have ratios between 0.6 and 1.0. This could either reflect direct melting of the lithospheric mantle due to conduction of heat from the asthenospheric source or, more probably, mixing between partial melts of these two sources. A change from lithosphere- to asthenosphere-signatures has been recognized in several flood basalt sequences in Antarctica (Storey & Alabaster 1991), Siberia (Lightfoot *et al.* 1993) and the southern Paraná (Peate & Hawkesworth 1996). The wide range of Nb/La ratios in the alkaline mafic rocks may also reflect generation by mixing of melts from different sources.

The group I dolerites have initial εNd_i values of about $+4$ and $+3$ that reflect the influence of a source that is moderately depleted, and whose isotopic composition is close to that of the PREMA mantle reservoir at 300 Ma ($\varepsilon Nd \geq 5$; Stein & Hofmann 1994). It also correlates with values for OIB suggesting the existence of an asthenospheric mantle source. The εNd_i values between 0 and -1 of the group II samples point to a mildly enriched source, and the signature may well represent crustal contamination (e.g. Griselin *et al.* 1997).

The depleted mantle source characteristic for group I dolerites conflicts with their incompatible trace-element patterns, which suggest derivation from an enriched mantle source. Therefore, the possibility of re-enrichment of an originally depleted source has to be considered. Magmatic events documented by intrusion of regional dyke swarms at 1180 Ma along the Protogine Zone and at 950 Ma in Blekinge, east of Scania (Gorbatschev *et al.* 1987; Johansson & Johansson 1990; Solyom *et al.* 1992, Söderlund 1999), imply Proterozoic depletion of the upper mantle below the thick crust of the southern Fennoscandian Shield. Caledonian subduction and continental collision between Baltica and eastern Avalonia during the Ordovician and Silurian (cf. Katzung 2001) may have led to a regional metasomatic overprint of the lithospheric mantle by LILE-enriched fluids for which some evidence may be present in the trace-element characteristics of the Permo-Carboniferous dykes in Scania. Radiogenic ingrowth, however, needs more time than the relatively short period between the enrichment process and the melt generation – especially for Nd.

Regional and tectonic implications

Based on palaeomagnetic data, the dolerites appear to have been intruded during Late Carboniferous (Silesian) times, while the alkaline rocks seem to be younger and are supposed to have a Permo-Triassic age (Bylund 1974). K–Ar dating was carried out for different types of the NW-trending dykes yielding a reliable isochron age of 294 ± 4 Ma for the dolerites intersecting the Palaeozoic rocks (Klingspor 1976). Modal ages between 306 and 416 Ma were obtained for dolerite dykes cutting the Precambrian basement but can be rejected because of the suspected capture of radiogenic

argon from the granitoid wallrocks. Slightly younger ages are suggested for the alkaline mafic rocks (Tolånga: 278 ± 7 Ma; Torpa Klint: 244 ± 3 Ma) and the trachytes (Torpa Klint: 293 ± 4 Ma; Dalby: 284 ± 4 Ma; Kullen: 251 ± 4 Ma). Based on field observations and considering the likely evolution in magma chemistry with progressive rifting, which often starts with alkaline melt production followed by generation of transitional or tholeiitic magmas, Obst (1999) proposed that the alkaline mafic dykes and the trachytic intrusions are probably older than the dolerite dykes. This assumption is weakly supported by results of Timmerman (pers. comm. 2001), who obtained $^{40}Ar/^{39}Ar$ ages of 287 ± 2 Ma (plagioclase phenocrysts) for a dolerite dyke exposed in the Hardeberga quarry in central Scania and 313 ± 11 Ma (hornblende microphenocrysts) for a lamprophyric dyke (spessartite) from NW Scania.

The uncertainties with respect to the ages of the alkaline mafic rocks of the Scania dyke swarm make it difficult to compare them with geochemically similar igneous rocks of the Permo-Carboniferous NW European magmatic province. The more precisely dated Scania tholeiites, however, can be usefully compared with tholeiitc rocks in the UK, Sweden and Germany of the same Late Carboniferous age, *c.* 300 Ma, to arrive at a simplified petrogenetic model (see also Neumann *et al.* 2004).

Scottish dolerite dykes and sills

A genetic link between the Swedish and Scottish dyke swarms and the dykes of the Oslo region was proposed by Hjelmqvist in 1939. Ernst & Buchan (1997) suggest that these dykes were all linked together by a plume head north of the Danish peninsula Jutland. Obst (1999) proposed a magmatic centre in the Kattegat (Fig. 1), supported by the fact that the major Oslo Graben dyke swarm does not trend directly to the postulated plume head north of Jutland, but rather SSE along the Swedish coast. In addition, a positive gravity anomaly, indicative of a presence of a large mafic body in the lower crust (although of indeterminate age), is centred on Silkeborg (Jutland), close to the possible Kattegat location.

The Scottish Permo-Carboniferous dolerite dyke swarm is extensive, with individual dykes up to 130 km in length and up to 45 m wide. In the Midland Valley they trend approximately E–W, whereas further north the swarm swings to roughly ENE–WSW, perhaps reflecting the regional Caledonian trend of their host rocks (Dunham & Strasser-King 1982). The E–W-trending dykes in the Midland Valley are mainly quartz-bearing tholeiites (Macdonald *et al.* 1981). The majority of these dykes and accompaining sills were erupted at about 300 ± 5 Ma (Timmerman 2004; Wilson *et al.* 2004).

The major- and trace-element characteristics of the Scotland tholeiites are very similar to those of the Scania tholeiites, reflecting derivation from similar trace-element-enriched mantle sources and fractional crystallization processes. The Mg-numbers vary in both suites between 60 and 30. Samples of both dyke swarms often follow nearly identical trends in bivariate plots; only minor differences are visible, e.g. for Ni (Fig. 11). The TiO_2 concentrations in the Scottish tholeiites are similar to those of the Scania dolerite I. The K_2O concentrations of the Scottish dykes scatter more probably reflecting crustal contamination or secondary alteration of some of the samples. There is no separation into two groups, as is possible for the Scania dolerites, except in the La–Sm diagram, where two different trends are clearly outlined (Fig. 12). The separation of the Scottish tholeiites is also suggested by the distribution in the Th/Ta v. Nb/La plot (Fig. 12), in which one half of the samples have Nb/La ratios above 0.9 similar to the group I dolerites of Scania, while the other half has lower values mostly coupled with higher Th/Ta ratios, as typical for the group II dolerites of Scania. This suggests source heterogeneities (magma mixing?) for the Scottish dolerites or is at least indicative of some crustal influence on the tholeiitic magmas. The geochemical characteristics of the important Whin Sill in northern England are also very similar to the Scottish tholeiites, plotting in the same array (Fig. 11).

Dolerite sills in Västergötland

Extensive dolerite sills are not only known from the UK sector of the NW European magmatic province but also from southern central Sweden, e.g. at Billingen, Kinnekulle, Halleberg and Hunneberg in Västergötland (Fig. 1), where they intrude Lower Palaeozoic sediments. Recently, dolerite dykes of inferred Permian age have been discovered south of Lake Vättern (Gorbatschev pers. comm. 1999), which could be considered to be the feeder dykes of the Västergötland sills. The sills are of approximately the same age as the dolerite dykes in Scania; new Ar–Ar analyses suggest an age of about 300 Ma (Timmerman 2004).

The results of geochemical analyses of the Kinnekulle and Hunneberg dolerites can be compared with the geochemistry of the Scania dolerites to evaluate mantle heterogeinities

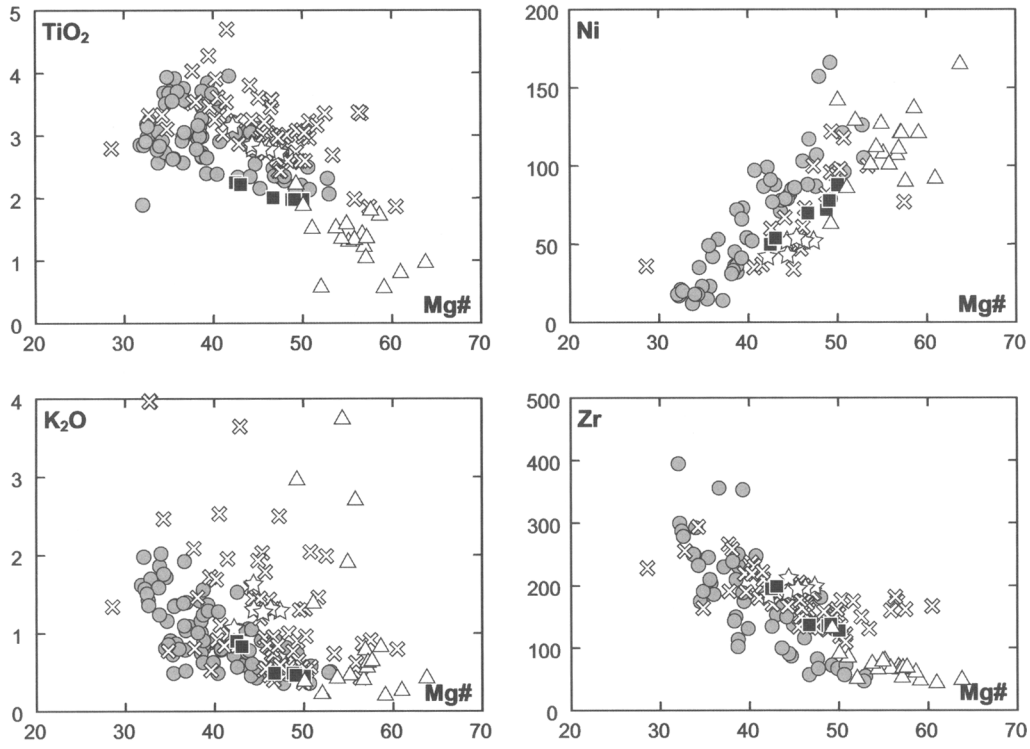

Fig. 11. Selected bivariate plots of major (wt%) and trace (ppm) elements v. Mg number show geochemical differences or common characteristics between tholeiites from different positions within the NW and central European magmatic province. Scania dolerite dykes, grey circles (data: this study and Obst 1999); Scotland dolerite dykes, white crosses (Macdonald *et al.* 1981); Whin dolerite sill, white stars (Kela *et al.* pers. comm.); Västergötland dolerite sills, black squares (data: this study); Rügen basalts and dolerite dykes/sills, white triangles (Kramer 1977, 1988).

below the southern Fennoscandian Shield. The Västergötland sill samples mostly follow the same trends as the Scania dykes in bivariate element plots, but the Kinnekulle dolerites have higher Mg numbers than those from Hunneberg (Fig. 11). The Västergötland sills are enriched in the whole range of incompatible trace elements; the normalized trace and REE pattern of the Kinnekulle samples are similar to the most primitive Scania tholeiites suggesting similar melt generation processes from a similar source in the upper mantle (Fig. 13). The patterns of the Hunnberg samples are more enriched in incompatible trace elements and show a negative trough at Nb–Ta implying crustal contamination.

Rügen tholeiites

South of the Fennoscandian Shield, large amounts of basaltic magma and anatectic crustal melts were emplaced in the North German Basin (Fig. 1) in a short time interval between 300 and 297 Ma (Breitkreuz & Kennedy 1999). The results of petrogenetic studies of magmatic rocks drilled in the eastern part of the North German Basin are summarized by Marx *et al.* (1995) and Benek *et al.* (1996). The Permo-Carboniferous sequence in boreholes up to 8000 m deep mainly consists of continental clastic sediments in which volcanic rocks with a total thickness of more than 2360 m are interbedded. While the southern part of the basin is dominated by intermediate–acid volcanic series, the NE part (especially the island of Rügen) is characterized predominantly by basaltic lava flows and tuffs of four eruptive periods. These volcanic rocks are accompanied by many cogenetic dolerite sills and dykes, which either are aphyric or olivine/pyroxene- or plagioclase-porphyritic. Their thickness ranges from a few centimetres to 145 m, but most of them are less than 10 m thick. The total

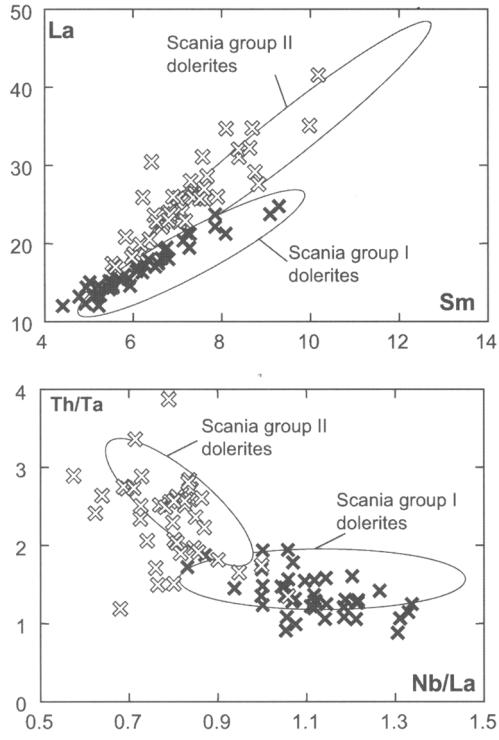

Fig. 12. The Scottish dolerite dykes (crosses) show two distinct trends in the La–Sm and Th/Ta–Nb/La diagrams similar to the Scania dolerite dykes (elliptic arrays), implying similar source heterogeneities or magma mixing and crustal contamination.

thickness of the intrusions reaches 600–1000 m in some of the boreholes (Korich & Kramer 1994).

Kramer (1977, 1988) has characterized the Rügen basalts as olivine tholeiites. Geochemical variations due to fractional crystallization are minor, but samples with spinel inclusions in orthopyroxene show the highest concentration of Cr (Korich & Kramer 1994). The Rügen tholeiites have mostly higher Mg-numbers than the Scania tholeiites, ranging between 65 and 50, and their TiO_2 concentrations are rather low (0.5–2%) compared to the tholeiites from other occurrences of the Permo-Carboniferous NW European magmatic province (Fig. 11). The geochemical characteristics of the Rügen tholeiites are similar to that of N-type MORB, as suggested by a rather flat pattern in the mantle-normalized trace-element and chondrite-normalized REE plots (Fig. 13). The general low concentrations of incompatible elements and positive εNd_i values of about +5 (Kramer pers. comm.) imply a depleted mantle source at a relatively high degree of partial melting, while the Scania tholeiitic dolerites represent melts of (re-)enriched mantle sources as discussed above. The relatively low Th/Ta ratios of the less altered samples of the Rügen tholeiites further indicate that they have not experienced much crustal contamination compared to the Scania tholeiites, especially those of group II. Secondary alteration, however, has affected the concentrations of mobile elements such as K, Ba, Rb and Cs, as indicated by positive deviations in the mantle-normalized trace-element pattern (Fig. 13).

Towards the south of the island of Rügen, within the North German Basin, the drilled

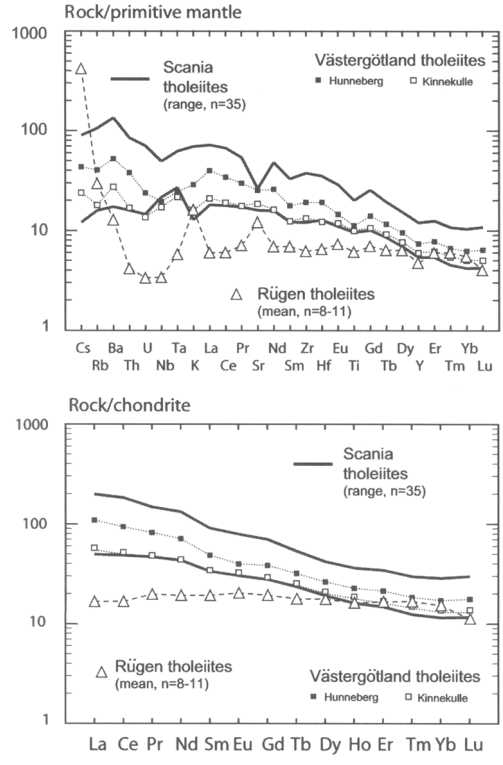

Fig. 13. Normalized trace-element patterns of the Västergötland dolerites (data: this study) are enriched in the whole range of incompatible elements similar to the Scania dolerites, while the Rügen basalts (data from Benek *et al.* 1996) have patterns similar to those of ocean-floor tholeiites (with the exception of Cs, Rb and Ba) suggesting a depleted mantle source and a relatively high degree of partial melting. The positive K anomaly and the relatively high Cs, Ba and Rb concentrations of the Rügen tholeiites are probably due to secondary alteration of the lava flows. Normalization factors are from McDonough & Sun (1995).

tholeiitic lavas have relatively enriched trace-element patterns, and the volcanic succession is more and more dominated by intermediate–acid rocks generated by antectic melting of the crust (Fig. 14). Mg-rich andesites in E Brandenburg, however, have geochemical characteristics typical of calc-alkaline rocks, probably generated at greater depths than the MORB- and continental-type tholeiites of Rügen and the adjacent mainland (Benek *et al.* 1996).

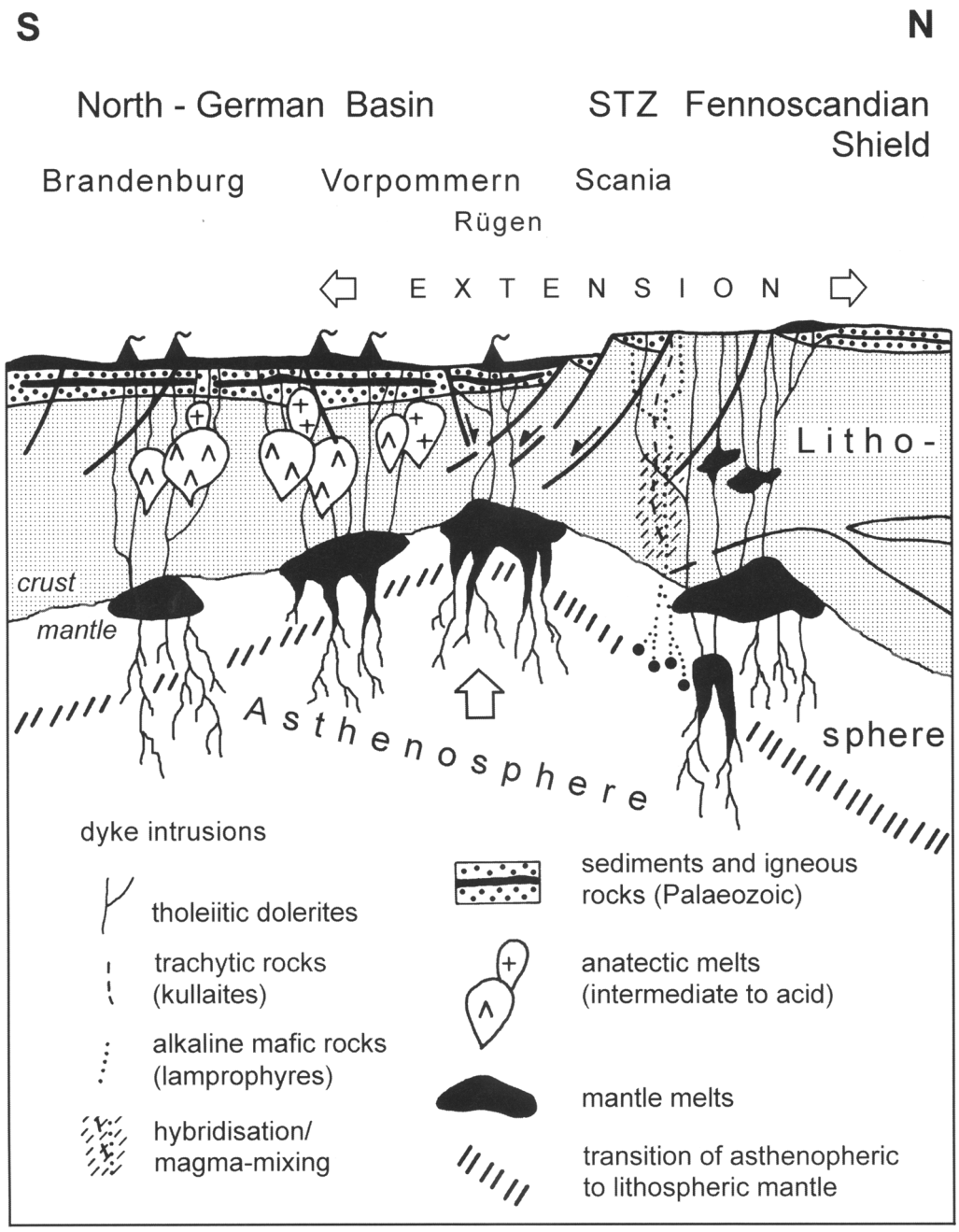

Fig. 14. Sketch (not to scale) of the tectono-magmatic processes that led to the formation of an intra-continental rift between Southern Sweden and NE Germany during Permo-Carboniferous times.

Conclusions

After the end of the Variscan Orogeny the regional tectonic regime in Central Europe changed, indicating the beginning of the break-up of the supercontinent Pangaea. Compressive tectonism was followed by extensional processes, which had already existed in the NW foreland of the Variscan Orogen since the Lower Carboniferous (e.g. indicated by extensive magmatism in the British Isles). Large-scale crustal extension is documented by the formation of regional dyke swarms in Scotland, the Oslo region and Scania, and also by the volcanic rocks piled up in the basins and half-grabens, e.g. in the North German Basin.

Lithospheric stretching induced pressure-release melting of ascending mantle material on a large scale in southern Sweden and northern Germany during Late Carboniferous–Permian times. The alkaline mafic dykes in Scania may represent the first melts generated at a very low degree of partial melting of a metasomatized mantle source (high concentrations of alkalies, Ba, Sr, Nb, P and CO_2), but this has to been proved by more precise age determinations. Increasing extension and upwelling of the asthenosphere promoted the generation of tholeiitic melts at higher degrees of partial melting from mildly depleted mantle sources indicated by the positive εNd_i values of the Scania group I dolerites ($+4$ to $+3$, this study) and the Rügen tholeiites (*c.* $+5$, Kramer pers. comm.). They intruded, and partly extruded, at the southern margin of the Fennoscandian Shield, where a large number of pre-existing faults could have been easily activated and opened by the rising magmas (Fig. 14).

The Scania dolerites forming the regional dyke swarm show enrichment in incompatible trace elements typical for continental tholeiites, while the Rügen basalts have mantle-normalized trace-element patterns that are similar to oceanic tholeiites. This most probably reflects heterogeneities in the upper-mantle sources of the magmas. Thus, the geochemical characteristics of the Scania dolerites, especially those of group I, either indicate re-enrichment of a sublithospheric magma source, probably due to Caledonian subduction and collision processes between the palaeocontinents of Baltica and Avalonia during Ordovician and Silurian times, or interaction of rising asthenosphere-derived melts (positive peak at Nb–Ta; Nb/La ratios mostly >0.9; εNd_i values about $+4$ and $+3$) with the subcontinental lithosphere, which is rather thick below the Fennoscandian Shield (Fig. 2b). Generation from, and/or increasing mixing with melts from, the lithospheric mantle is indicated by the geochemical characteristics of Scania group II dolerites (minor positive peak or negative trough at Nb–Ta; Nb/La ratios mostly <0.9; εNd_i values about 0 and -1). Increasing ratios of Th/Ta and decreasing ratios of Nb/U further suggest crustal contamination of dolerite samples from this group; this may have been also affected some samples of the group I dolerites.

The low Th/Ta ratios of the less altered Rügen basalts indicate that these melts were nearly unaffected by crustal contamination on their fast ascent through the relatively thin crust at the northern margin of the North German Basin, compared to those magmas that penetrated the thick crust of the Fennoscandian Shield. The generally low concentrations of incompatible trace elements suggests that these relatively less fractionated melts (Mg-numbers between 65 and 50, positive Sr anomaly) were generated in a position close to the axis of a rift, as in the Red Sea today. The Scania magmas, however, intruded in a more marginal rift position, and have been stored in magma chambers before intrusion, as suggested by the extended crystal fractionation (Mg-numbers between 55 and 30). In this context it is consistent that the most primitive dolerites of group I ($MgO > 6\%$, positive Nb–Ta anomaly and positive or no Sr peak) occur at the southern margin of the Scania dyke swarm.

The question of whether the tholeiitic magmas of Scania were primarily fed from a plume head or a magmatic centre in the Kattegatt contemporaneous with tholeiitic magmas in Scotland and NE England (tholeiitic dykes and sills) or the Oslo Gaben (tholeiitic dykes and lavas at Krokskogen; see Neumann *et al.* 2004) is still unsolved. Similar geochemical characteristics or structural indicies are not enough to give a clear answer. Studies of flow directions within the dykes by mean of anisotropic susceptibility measurements may help in the future to solve this problem.

We gratefully thank U. Siewers and his colleagues (BGR Hannover) who made the geochemical analyses possible, and A. Kronz (Universität Göttingen) for his support during microprobe measurements. The manuscript has been improved by critical comments from M. Wilson (University of Leeds), S. Foley (Universität Mainz), R. MacDonald (University of Lancaster) and Else-Ragnhild Neumann (University of Oslo).

References

ANDERSON, D.L. 1994. Superplumes or supercontinents? *Geology*, **22**, 39–42.

ARMSTRONG, J.T. 1995. CITZAF: A package of correction programs for the quantitative electron microbeam x-ray analysis of thick polished materials, thin films, and particles. *Microbeam Analysis*, **4**, 177–200.

ARNDT, N.T. & CHRISTENSEN, U. 1992. The role of lithospheric mantle in continental flood volcanism: thermal and geochemical constraints. *Journal of Geophysical Research*, **97**, 10 967–10 981.

BENEK, R., KRAMER, W. MCCANN, T., SCHECK, M., NEGENDANK, J.F.W., KORICH, D., HUEBSCHER, H.-D. & BAYER, U. 1996. Permo-Carboniferous magmatism of the Northeast German Basin. *Tectonophysics*, **266**, 379–404.

BERGSTRÖM, J. 1985. Zur tektonischen Entwicklung Schonens (Südschweden). *Zeitschrift für Angewandte Geologie*, **31**, 277–280.

BERTHELSEN, A. 1992. From Precambrian to Variscan Europe. *In*: BLUNDELL, D., FREEMAN, R. & MUELLER, ST. (eds) *A Continent Revealed. The European Geotraverse*. University Press, Cambridge, 153–164.

BLUNDELL, D. 1992. Integrated lithospheric cross section. *In*: BLUNDELL, D., FREEMAN, R. & MUELLER, ST. (eds) *A Continent Revealed. The European Geotraverse*. University Press, Cambridge, 102–109.

BREITKREUZ, C. & KENNEDY, A. 1999. Magmatic flare-up at the Carboniferous/Permian boundary in the NE German Basin revealed by SHRIMP zircon ages. *Tectonophysics*, **302**, 307–326.

BYLUND, G. 1974. Palaeomagnetism of dykes along the southern margin of the Baltic Shield. *Geologiska Föreningens i Stockholm Förhandlingar*, **96**, 231–235.

CAMPBELL, I.H. & GRIFFITHS, R.W. 1990. Implications of a mantle plume structure for the evolution of flood basalts. *Earth and Planetary Science Letters*, **99**, 79–93.

DADLEZ, R. 1997. Seismic profile LT-7 (northwest Poland): geological implications. *Geological Magazine*, **134**, 653–659.

DUNHAM, A.C. & STRASSER-KING, V.E.H. 1982. Late Carboniferous intrusions of northern Britain. *In*: SUTHERLAND, D.S. (ed.) *Igneous Rocks of the British Isles*. J Wiley, Chichester, 277–294.

ERNST, R.E. & BUCHAN, K.L. 1997. Giant radiating dyke swarms: Their use in identifying pre-mesozoic large igneous provinces and mantle plumes. *In*: MAHONY, J.J. & COFFIN, M.F. (eds) *Large Igneous Provinces: Continental, Oceanic, and Planetary Flood Volcanism*. American Geophysical Union, Geophysical Monograph, **100**, 297–333.

FOLEY, S. 1992. Vein-plus-wall-rock melting mechanisms in the lithosphere and the origin of potassic alkaline magmas. *Lithos*, **28**, 435–453.

FRANCIS, E.H. 1978. The Midland valley as a rift, seen in connection with the late Palaeozoic European rift system. *In*: RAMBERG, I.B. & NEUMANN, E.-R. (eds) *Tectonics and Geophysics of Continental Rifts*. Reidel, Dordrecht, 133–147.

FRANCIS, E.H. 1991. Carboniferous–Permian igneous rocks. *In*: CRAIG, G.Y. (ed.) *The Geology of Scotland*. Geological Society, London, 393–415.

FROST, B.R. & LINDSLEY, D.H. 1991. Occurrence of iron-titanium oxides in igneous rocks. *In*: LINDSLEY, D.H. (ed.) *Oxide Minerals; Petrologic and Magnetic Significance. Reviews in Mineralogy*, **25**, 433–468.

GOSSLER, J., KIND, R., SOBOLEV, S.V., KÄMPF, H., WYLEGALLA, K. & STILLER, M. 1999. Major crustal features between the Harz Mountains and the Baltic Shield derived from receiver functions. *Tectonophysics*, **314**, 321–333.

GORBATSCHEV, R., LINDH, A., SOLYOM, Z., LAITAKARI, I., ARO, K., LOBACH-ZHUCHENKO, S.B., MARKOV, M.S., IVLIEV, A.I. & BRYHNI, I. 1987. Mafic dyke swarms of the Baltic Shield. *In*: HALLS, H.C. & FAHRIG, W.F. (eds) *Mafic Dyke Swarms*. Geological Association of Canada, Special Paper, **34**, 361–372.

GRISELIN, M., ARNDT, N.T. & BARAGAR, W.R.A. 1997. Plume–lithosphere interaction and crustal contamination during formation of Coppermine River basalts, Northwest Territories. *Canadian Journal of Earth Sciences*, **34**, 958–975.

HADDING, A. 1916. Iakttagelser över melafyrerna i Tolångatrakten. *Lunds Universitets Årsskrift., N.F., Avd. 2*, **13**, 1–37.

HAWKESWORTH, C.J., MANTOVANI, M.S.M. & PEATE, D.W. 1988. Lithosphere remobilisation during Parana CFB magmatism. *In*: MENZIES, M.A. & COX, K.G. (eds) *Oceanic and Continental Lithosphere: Similarities and Differences. Journal of Petrology*, Special volume, 205–223.

HERGT, J.M., PEATE, D.W. & HAWKESWORTH, C.J. 1991. The petrogenesis of Mesozoic Gondwana low Ti-flood basalts. *Earth and Planetary Science Letters*, **105**, 134–148.

HENKEL, H. & SUNDIN, N.O. 1979. Magnetisk undersökning av två korsande diabasgangar i Skåne. *Sveriges Geologiska Undersökning, Geofysisk Rapport*, **7902**, 1–13.

HENNIG, A. 1899. Kullens kristallinska bergarter. II. Den postsiluriska gångformationen. *Lunds Universitets Årsskrift*, **35**, 1–34.

HIRSCHMANN, M.M. & STOLPER, E.M. 1996. A possible role for garnet pyroxenite in the origin of the 'garnet signature' in MORB. *Contributions to Mineralogy and Petrology*, **124**, 185–208.

HJELMQVIST, S. 1930. Kullait von Dalby. *Geologiska Föreningens i Stockholm Förhandlingar*, **52**, 247–268.

HJELMQVIST, S. 1939. Some post-silurian dykes in Scania and problems suggested by them. *Sveriges Geologiska Undersökning, Ser. C*, Nr. 430, **33**, 1–32.

HOFMANN, A.W., JOCHUM, K.P., SEIFART, M. & WHITE, W.M. 1986. Nb and Pb in oceanic basalts: new constraints on mantle evolution. *Earth and Planetary Science Letters*, **79**, 33–45.

HOFFMANN, N., JÖDICKE, H., FLUCHE, B., JORDING, A. & MÜLLER, W. 1998. Modellvorstellungen zur Verbreitung potentieller präwestfalischer Erdgas-Muttergesteine in Norddeutschland – Ergebnisse

neuer magnetotellurischer Messungen. *Zeitschrift für Angewandte Geologie*, **44**, 140–158.

JOHANSSON, L. & JOHANSSON, Å. 1990. Isotope geochemistry and age relationships of mafic intrusions along the Protogine Zone, southern Sweden. *Precambrian Research*, **48**, 395–414.

KLINGSPOR, I. 1976. Radiometric age-determination of basalts, dolerites and related syenite in Skåne, southern Sweden. *Geologiska Föreningens i Stockholm Förhandlingar*, **98**, 195–216.

KATZUNG, G. 2001. The Caledonides at the southern margin of the East European Craton. *Neues Jahrbuch für Geologie und Paläontologie, Abhandlungen*, **222**, 3–53.

KORICH, D. & KRAMER, W. 1994. Permosilesische Magmatite im Untergrund von Rügen und der östlich angrenzenden Ostsee. *Zeitschrift für Geologische Wissenschaften*, **22**, 249–256.

KRAMER, W. 1977. Vergleichende geochemisch-petrologische Untersuchungen an permosilesischen basischen Magmatiten der Norddeutsch-Polnischen Senke und ihre geotektonische Bedeutung. *Zeitschrift für Geologische Wissenschaften*, **5**, 7–20.

KRAMER, W. 1988. Magmengenetische Aspekte der Lithosphärenentwicklung. Geochemisch-petrologische Untersuchungen basaltoider variszischer Gesteinsformationen sowie mafischer und ultramafischer Xenolithe im nordöstlichen Zentraleuropa. *Schriftenreihe Geologische Wissenschaften*, **26**, 1–136.

LEAKE, B.E. & 21 others. 1997. Nomenclature of amphiboles: Report of the Subcommittee on Amphiboles of the International Mineralogical Association Commission on New Minerals and Mineral Names. *Canadian Mineralogist*, **35**, 219–246.

LE MAITRE, R.W. (ed.). 2002. *A Classification of Igneous Rocks and Glossary of Terms. Recommendations of the International Union of Geological Sciences Subcommission on the Systematics of Igneous Rocks*. Cambridge University Press, Cambridge.

LIGHTFOOT, P.C., HAWKESWORTH, C.J., HERGT, J.M. & NALDRETT, A.J. 1993. Remobilisation of the continental lithosphere by a mantle plume: major-, trace-element, and Sr-, Nd- and Pb-isotope evidene from picritic and tholeiitic lavas of Norilsk District, Sibirian Trap, Russia. *Contributions to Mineralogy and Petrology*, **114**, 171–188.

MACDONALD, R., GOTTFRIED, D., FARRINGTON, M.J., BROWN, F.W. & SKINNER, N.G. 1981. Geochemistry of a continental tholeiite suite: late Palaeozoic quartz dolerite dykes of Scotland. *Transactions of the Royal Society of Edinburgh: Earth Sciences*, **72**, 57–74.

MARX, J., HUEBSCHER, H.-D., HOTH, K., KORICH, D. & KRAMER, W. 1995. Vulkanostratigraphie & Geochemie der Eruptivkomplexe. *In*: PLEIN, E. (ed.) *Stratigraphie von Deutschland I – Norddeutsches Rotliegendbecken*. Courier Forschungsinstitut Senckenberg, **183**, 54–83.

MCDONOUGH, W.F. & SUN, S. 1995. The composition of the Earth. *Chemical Geology*, **120**, 223–253.

MEARNS, E.W. 1986. Sm–Nd ages for Norwegian garnet peridotites. *Lithos*, **19**, 269–278.

MENNING, M., WEYER, D., DROZDZEWSKI, G., AMEROM, H.W.J. VAN & WENDT, I. 2000. A Carboniferous time scale 2000: discussion and use of geological parameters as time indicators from Central and Western Europe. *Geologisches Jahrbuch Hannover, Reihe A*, **156**, 3–44.

NEUMANN, E.-R. 1994. The Oslo Rift: P–T relations and lithospheric structure. *Tectonophysics*, **240**, 59–172.

NEUMANN, E.-R., WILSON, M., HEEREMANS, M., SPENCER, E.A., OBST, K., TIMMERMAN, M.J. & KIRSTEIN, L. 2004. Carboniferous–Permian rifting and magmatism in Southern Scandinavia, the North Sea and northern Germany: a review. *In*: WILSON, M., NEUMANN, E.-R., DAVIES, G.R., TIMMERMAN, M.J., HEEREMANS, M. & LARSEN, B.T. (eds) *Permo-Carboniferous Magmatism and Rifting in Europe*. Geological Society, London, Special Publications, **223**, 11–40.

OBST, K. 1999. Die permosilesischen Eruptivgänge innerhalb der Fennoskandischen Randzone (Schonen und Bornholm) – Untersuchungen zum Stoffbestand, zur Struktur und zur Genese. *Greifswalder Geowissenschaftliche Beiträge*, **7/1999**, 5–121.

OBST, K. 2000. Permo-Carboniferous dyke magmatism on the Danish island Bornholm. *Neues Jahrbuch für Geologie und Paläontologie, Abhandlungen*, **218**, 243–266.

OBST, K. & KATZUNG, G. 2004. Spatial distribution and emplacement features of Permo-Carboniferous dykes at the southwestern margin of the Fennoscandian Shield. *In*: *Proceedings of the 4th International Dyke Conference, South Africa*. Balkema, Rotterdam.

PASCAL, C., CLOETINGH, S.A.P.L. & DAVIES, G.R. 2004. Asymmetric lithosphere as the cause of rifting and magmatism in the Permo-Carboniferous Oslo Graben. *In*: WILSON, M., NEUMANN, E.-R., DAVIES, G.R., TIMMERMAN, M.J., HEEREMANS, M. & LARSEN, B.T. (eds) *Permo-Carboniferous Magmatism and Rifting in Europe*. Geological Society, London, Special Publications, **223**, 139–156.

PEATE, D.W. & HAWKESWORTH, C.J. 1996. Lithospheric to asthenospheric transition in low-Ti flood basals from southern Parana. *Brazilian Chemical Geology*, **127**, 1–24.

PENG, Z.X., MAHONEY, J.J., HOOPER, P., HARRIS, C. & BEANE, J. 1994. A role for lower continental crust in flood basalt genesis? Isotopic and incompatible element study of the lower six formations of the western Deccan Traps. *Geochimica et Cosmochimica Acta*, **58**, 267–288.

RAMBERG, I.B. & LARSEN, T.B. 1978. Tectonomagmatic evolution. *In*: DONS, J.A. & LARSEN, T.B. (eds) *The Oslo Palaeorift. A Review and Guide to Excursions. Norges Geologiske Undersøkelse*, **337**, 105–124.

ROCK, N.M.S. 1991. *Lamprophyres*. Blackie, London.

SGU 1998. *Skånes berggrund*. Skala 1:700 000. Sveriges Geologiska Uudersökning, Lund.

SÖDERLAND, U. 1999. *Geochronology of tectonothermal events in the parantochthonous eastern segment*

of the Sveconorweisglan (Grenvillian) orogen, southwest Sweden. PhD thesis, University of Lund.

SOLYOM, Z., LINDQVIST, J.-E. & JOHANSSON, I. 1992. The geochemistry, genesis, and geotectonic setting of Proterozoic mafic dyke swarms in southern and central Sweden. *Geologiska Föreningens i Stockholm Förhandlingar*, **114**, 47–65.

STEIN, M. & HOFMANN, A.W. 1994. Mantle plumes and episodic crustal growth. *Nature*, **372**, 63–68.

STOREY, B.C. & ALABASTER, T. 1991. Tectonomagmatic controls on Gondwana break-up models: evidence from the proto-Pacafic margin of Antarctica. *Tectonics*, **10**, 1274–1288.

SUNDVOLL, B. & LARSEN, B.T. 1995. Architecture and early evolution of the Oslo Rift. *Tectonophysics*, **240**, 173–189.

THOMPSON, R.N., MORRISON, M.A., DICKIN, A.P. & HENDRY, G.L. 1983. Continental flood basalts ... arachnids rule ok? *In*: HAWKESWORTH, C.J. & NORRY, M.J. (eds) *Continental Basalts and Mantle Xenoliths*. Shiva, Nantwich, 158–185.

THYBO, H., KIORBOE, L.L., MOELLER, C., SCHÖNHARTING, G. & BERTHELSEN, A. 1990. Geophysical and tectonic modelling of EUGENO-S profiles. *In*: FREEMAN, R. & MUELLER, ST. (eds) *Sixth EGT Workshop: Data Compilations and Synoptic Interpretation*. European Science Foundation, Strasbourg, 93–104.

TIMMERMAN, M.J. 2004. Timing, geodynamic setting and characters of Permo-Carboniferous magmatism in the foreland of the Variscan Orogen, NW Europe. *In*: WILSON, M., NEUMANN, E.-R., DAVIES, G.R., TIMMERMAN, M.J., HEEREMANS, M. & LARSEN, B.T. (eds) *Permo-Carboniferous Magmatism and Rifting in Europe*. Geological Society, London, Special Publications, **223**, 41–74.

WHITE, R.S. & MCKENZIE, D.P. 1989. Magmatism at rift zones: the generation of volcanic continental margins and flood basalts. *Journal of Geophysical Research*, **94**, 7685–7730.

WILSON, M., NEUMANN, E.-R., DAVIES, G.R., TIMMERMAN, M.J., HEEREMANS, M. & LARSEN, B.T. 2004. Permo-Carboniferous magmatism and rifting in Europe: introduction. *In*: WILSON, M., NEUMANN, E.-R., DAVIES, G.R., TIMMERMAN, M.J., HEEREMANS, M. & LARSEN, B.T. (eds) *Permo-Carboniferous Magmatism and Rifting in Europe*. Geological Society, London, Special Publications, **223**, 1–10.

ZIEGLER, P.A. 1990. *Geological Atlas of Western and Central Europe* (2nd edn). Shell Internationale Petroleum Maatschappij, The Hague. Distributed by the Geological Society Publishing House, Bath.